Quarterly Reviews of Biophysics

cambridge.org/qrb

Determination of protein–protein interactions at the single-molecule level using optical tweezers

Wendy N. Sánchez[1,2], Luka Robeson[1], Valentina Carrasco[1], Nataniel L. Figueroa[3,4], Francesca Burgos-Bravo[5], Christian A. M. Wilson[1] and Nathalie Casanova-Morales[6]

[1]Biochemistry and Molecular Biology Department, Faculty of Chemistry and Pharmaceutical Sciences, Universidad de Chile, Santiago, Chile; [2]Department of Molecular Microbiology, Groningen Biomolecular Sciences and Biotechnology Institute, Faculty of Science and Engineering, University of Groningen, Groningen, The Netherlands; [3]Johannes Gutenberg-Universität Mainz, 55128 Mainz, Germany; [4]Helmholtz-Institut Mainz, GSI Helmholtzzentrum für Schwerionenforschung, 55128 Mainz, Germany; [5]Institute for Quantitative Biosciences, University of California, Berkeley, CA 94720, USA and [6]Facultad de Artes Liberales, Universidad Adolfo Ibáñez, Santiago, Chile

Review Article

Cite this article: Sánchez WN, Robeson L, Carrasco V, Figueroa NL, Burgos-Bravo F, Wilson CAM, Casanova-Morales N (2022). Determination of protein–protein interactions at the single-molecule level using optical tweezers. *Quarterly Reviews of Biophysics* **55**, e8, 1–17. https://doi.org/10.1017/S0033583522000075

Received: 19 January 2022
Revised: 23 June 2022
Accepted: 24 June 2022

Key words:
Protein-protein interaction; optical tweezers; Dudko-Hummer-Szabo model; force spectroscopy; binding parameters

Authors for correspondence: Christian A. M. Wilson, E-mail: yitowilson@gmail.com; Nathalie Casanova-Morales, E-mail: casa886@gmail.com

Abstract

Biomolecular interactions are at the base of all physical processes within living organisms; the study of these interactions has led to the development of a plethora of different methods. Among these, single-molecule (*in singulo*) experiments have become relevant in recent years because these studies can give insight into mechanisms and interactions that are hidden for ensemble-based (*in multiplo*) methods. The focus of this review is on optical tweezer (OT) experiments, which can be used to apply and measure mechanical forces in molecular systems. OTs are based on optical trapping, where a laser is used to exert a force on a dielectric bead; and optically trap the bead at a controllable position in all three dimensions. Different experimental approaches have been developed to study protein–protein interactions using OTs, such as: (1) refolding and unfolding in *trans* interaction where one protein is tethered between the beads and the other protein is in the solution; (2) constant force in *cis* interaction where each protein is bound to a bead, and the tension is suddenly increased. The interaction may break after some time, giving information about the lifetime of the binding at that tension. And (3) force ramp in *cis* interaction where each protein is attached to a bead and a ramp force is applied until the interaction breaks. With these experiments, parameters such as kinetic constants (k_{off}, k_{on}), affinity values (K_D), energy to the transition state $\Delta G^{\neq}$, distance to the transition state $\Delta x^{\neq}$ can be obtained. These parameters characterize the energy landscape of the interaction. Some parameters such as distance to the transition state can only be obtained from force spectroscopy experiments such as those described here.

Table of contents

State of the art 1
A general overview of binding methodologies 2
Measurement of forces to study binding in biochemical reactions 2
Experiments of binding at the single-molecule level 2
Optical tweezers 4

Detailed description of intermolecular interaction force experiments using OTs 5
Bead surface functionalization 5
Real-time intermolecular interaction in OTs 7
OT experiment 8

Data analysis/processing 11
Refolding and unfolding in *trans* interaction strategy 11
Constant force in *cis* interaction strategy 11
Force ramp in *cis* interaction strategy 12

Methodology to obtain the specific interaction forces between the molecules of interest 12

Conclusions 13

© The Author(s), 2022. Published by Cambridge University Press

State of the art

A general overview of binding methodologies

Life is based on molecular interactions, where binding of specific molecular partners is critical to the function of biological systems. These interactions can be characterized by binding parameters such as: the affinity (dissociation constant K_D) and kinetic dissociation (off-rate or k_{off}) or association (on-rate or k_{on}) constants; which give important information about the binding dynamics between molecules. This information is closely related to the energy landscape of the binding process (Tinoco *et al.*, 2013) and can be useful for drug development, where the first step is to study the binding of different compounds to a particular target.

Methods classically used to investigate biomolecular interactions are mostly performed in standard ensemble-based studies (or *in multiplo*), where population-average binding parameters are obtained due to the stochastic behavior of binding processes. Some of these methods are fluorescence studies, such as polarization changes in a tryptophan environment (Ghisaidoobe and Chung, 2014; Singha Roy *et al.*, 2014), or detecting changes in the emission of fluorescence-labeled proteins; surface plasmon resonance, where changes in light are measured while reflecting off functionalized gold surfaces (Misselwitz *et al.*, 1998); nanorheology, which measures the elastic properties of a protein (Casanova-Morales *et al.*, 2018*b*); and electrophoretic mobility shift assays, in which changes in displacement is measured in gels after binding (Fillebeen *et al.*, 2014); among many others. Most of these studies on protein–protein interactions focus on characterizing binding parameters using molecules in a solution, under thermal equilibrium, and free of external forces (O'Shannessy, 1994; Li *et al.*, 2007). The average binding parameters obtained by *in multiplo* techniques can often hide interesting interactions that can be observed at the single-molecule level (*in singulo*) (Bustamante, 2008).

In singulo studies have become increasingly popular in recent years because they can be used to follow the behavior of an individual molecule through time. Thus, it is possible to obtain not just the average behavior of many molecules, but rather the behavior of an individual of that population. This has opened a window into many cellular processes in which only a small subset of molecules participate (e.g. DNA transcription), and can exhibit behavior that is very different than that of the ensemble average. Thus, *in multiplo* studies do not portray a complete picture of the fluctuations that can arise in cellular processes (Bustamante, 2008) and can hide essential mechanisms at play in intermolecular interactions that can be identified with *in singulo* studies.

Measurement of forces to study binding in biochemical reactions

Another important advantage of *in singulo* studies is the possibility to apply and measure mechanical forces. Usually, reactions are studied by means of manipulating several thermodynamic parameters, such as: temperature (Baez *et al.*, 2012), chemical concentration (Casanova-Morales *et al.*, 2018*a*), and pressure (Akasaka *et al.*, 2013). All of these macroscopic variables may change the kinetic parameters of the reactions; the application of force can microscopically alter the same parameters. Since the very early studies of binding, there has been a clear relationship between forces and affinity. Antoine Lavoisier and Marie Anne Pierrette, in their seminal book *Elements of Chemistry*, use affinity and force indistinctly (Lavoisier, 1790). By focusing on force, the reaction coordinate becomes an easily quantifiable physical parameter, such as the end-to-end distance of a stretched molecule (Bustamante *et al.*, 2004; Tinoco, 2004).

In a physiological context, protein–protein interactions generally occur under non-equilibrium conditions and between molecules anchored to surfaces, such as the cell membrane or the extracellular matrix (Stout, 2001). Moreover, the bonds supporting protein–protein interactions *in vivo* can be in mechanical stress produced by either external (e.g. shear flow) or internal (e.g. actin cytoskeleton contraction) sources (Pollard and Borisy, 2003; Fournier *et al.*, 2010). For example, during tumor metastasis, cancer cell adhesion to the vascular endothelium is exposed to the hemodynamic force caused by blood flow. Additionally, during migration, cells tug on each other and exert traction forces on the molecular interactions that maintain cell–cell adhesion (Ananthakrishnan and Ehrlicher, 2007). It has long been recognized that forces control such molecular bonds by regulating their dissociation kinetics (Bell, 1978). Theoretical models and experimental observations have described a wide variety of mechanical responses in which the force applied to disrupt an interaction can accelerate (slip bond), slow down (catch bond),- or have no impact (ideal) on the bond dissociation (Dembo *et al.*, 1988; Zhu 2014). Interestingly, several studies have identified new classes of interactions in which the force-regulated bond dissociation is more complex, including dynamic catch bonds (Fiore *et al.*, 2014) and flex-bonds (Kim *et al.*, 2010). Experimentally, the force-dependent dissociation of two or more interacting proteins can be achieved by using single-molecule force spectroscopy techniques (described below), which have been widely employed to describe how mechanical cues regulate molecular interactions (Yuan *et al.*, 2000; Stangner *et al.*, 2013). Details about the energy landscape of the dissociation process can be extracted from these force-induced protein–protein unbinding studies, including the thermodynamics and kinetics of bond rupture, as well as the specificity of interaction between proteins (Stangner *et al.*, 2013; Burgos-Bravo *et al.*, 2018).

Experiments of binding at the single-molecule level

Several innovative methods have been used to monitor individual bond formation and dissociation, providing unique insights into molecular mechanisms. Techniques that allow direct visualization of single-molecule interactions without the application of force include fluorescence correlation spectroscopy and fluorescence cross-correlation spectroscopy. Techniques using force to manipulate single-binding events include laminar flow chambers (Alon *et al.*, 1995; Robert *et al.*, 2007) and molecular force spectroscopy. The most common force-based tools are biomembrane force probes (BFPs; Evans *et al.*, 1995; Merkel *et al.*, 1999), atomic force microscopy (AFM; Florin *et al.*, 1994; Lee *et al.*, 1994*b*; Hinterdorfer *et al.*, 1996), magnetic tweezers (MTs; Danilowicz *et al.*, 2005; Shang and Lee, 2007; Kilinc *et al.*, 2012), acoustic force spectroscopy (AFS; Sitters *et al.*, 2014), and optical tweezers (OTs; Nishizaka *et al.*, 1996; Rinko *et al.*, 2004; Litvinov *et al.*, 2005). In this article, we provide an overview of the different force-applying techniques used to study biomolecular interactions at the single molecule. Additionally, an extensive description of distinct biological assays that OTs enable is described, followed by a novel and detailed methodology to perform binding experiments using a compact and user-friendly OT instrument commercially known as miniTweezers (Smith *et al.*, 2003); see Fig. 1e.

https://doi.org/10.1017/S0033583522000075 Published online by Cambridge University Press

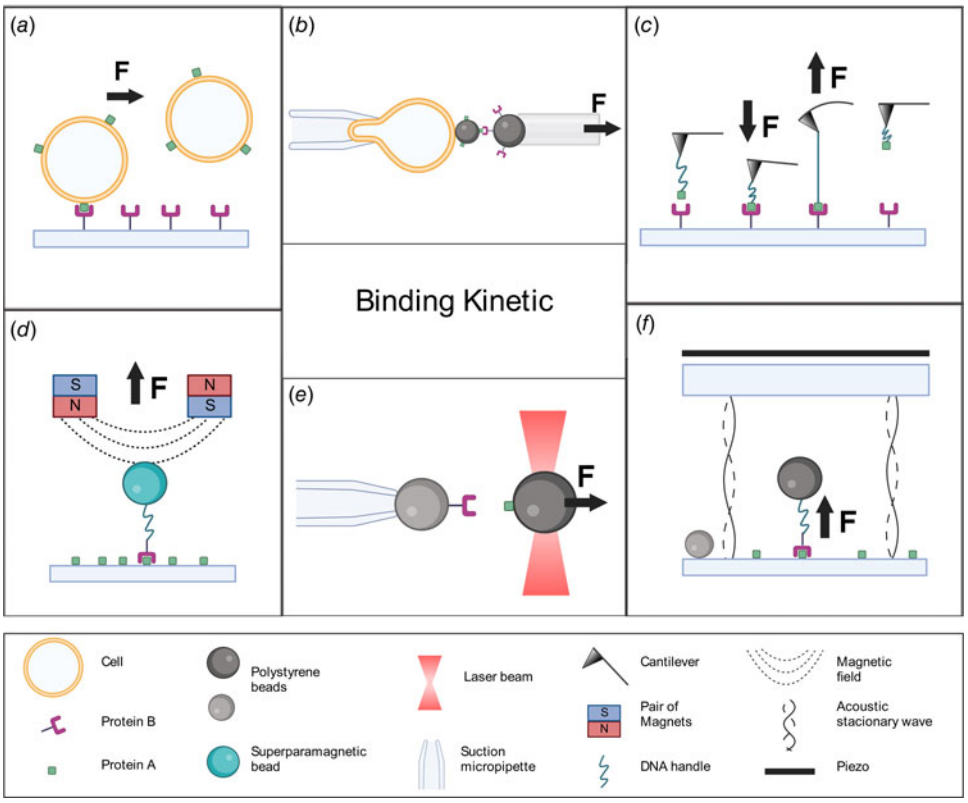


Fig. 1. Single-molecule force spectroscopy techniques. (*a*) Laminar flow chamber: a laminar flow exerts a force in the direction of the arrow causing rupture events between a ligand (protein A, green square) bounded to a cell, and a receptor (protein B, purple) coated to a surface. (*b*) BFP: a bead coated with ligands is attached to a transducer cell held by a suction micropipette. A second bead bearing receptors is brought into contact with the first bead and then retracted in the direction of the arrow, the deformation of the cell transducer caused by the rupture event is measured. (*c*) AFM: a cantilever bearing a ligand tethered to a dsDNA handle is allowed to bind a receptor-coated surface (arrow pointing down), during the retraction process (arrow pointing up) the bending of the cantilever caused by the strength of the interaction between the proteins is measured. (*d*) MTs: a superparamagnetic bead (in blue) bearing a receptor tethered to a dsDNA handle is manipulated with a magnetic field (dashed lines) caused by pairs of magnets. The bead is brought into a ligand-coated surface, and the binding force is measured during the retraction process as indicated by the arrow. (*e*) OTs: a ligand-functionalized bead is trapped and manipulated by light beams. The trapped bead is brought into contact with a receptor-functionalized bead held by a suction micropipette. During the retraction process (arrow direction), the interaction rupture force is measured. (*f*) AFS: a bead bearing a receptor tethered to a dsDNA handle is allowed to contact the bottom glass coated with ligands. The piezo element generates an acoustic wave that is reflected by the bottom glass (dashed curve), producing a standing wave. The bead exposed to this standing wave experiences a force (indicated by arrow) causing the rupture event. An immobilized bead at the bottom glass is used to determine the position of the bead experiencing force.

Laminar flow chambers

The basic principle of studying molecule interactions with laminar flow chambers consists of monitoring the trajectories of a receptor bound to a cell or particle along a ligand-coated surface in the presence of a laminar flow (Robert *et al.*, 2007; Zohra, 2021). The cell or particle is tethered to a surface and subjected to a hydrodynamic force (see Fig. 1*a*). The interaction frequency (e.g. the number of binding events per second), and the detachment kinetics (e.g. the fraction of particles remaining bound as a function of time after arrest) can be obtained from this assay (Pierres *et al.*, 2008). This approach resembles the *in vivo* conditions of several protein–protein interactions, such as the binding between endothelial cell selectins and their glycoprotein ligands on leukocytes. Selectin interactions were the first molecules studied at the single-bond level with laminar flow chambers. Here, a rapid dissociation constant of $1\ s^{-1}$ was reported for the binding between selectins and P-selectin glycoprotein ligand 1 (PSGL-1; Alon *et al.*, 1995). This technique has been widely used to investigate cellular processes that involve protein–protein interactions (e.g. cell adhesion or migration), respond to shear forces (Polacheck *et al.*, 2011; Shemesh *et al.*, 2015). Additionally, this method has also been implemented to characterize single-molecule interactions, for example, between streptavidin and biotin (Pierres *et al.*, 2002). See Fig. 1*a*.

Single-molecule force spectroscopy techniques

Biomembrane force probe. BFP is a versatile method that can be used in a wide range of forces (10^{-1}–10^{3} pN) and loading rates (1–10^{6} pN s^{-1}) (Gourier *et al.*, 2008). This technique consists of using cell-sized membrane capsules like vesicles, liposomes, or red blood cells (RBCs) as force transducers (Sung *et al.*, 1986; Shao 2004). The membrane capsule is held in place by a suction micropipette, and a protein-coated bead can be attached to the force probe (Ungai-Salánki *et al.*, 2019). This bead can then form the bond to be studied with a target, such as another bead, a vesicle, or a living cell, also held in place. The force measurements consist of automatized retraction–contraction cycles between the ligand-functionalized probe (i.e. bead connected to the soft spring RBCs) and target-bearing receptors (Gourier *et al.*, 2008). During the retraction step, the bond is subjected to a tension force that stretches the transducer. This deformation is measured by precise video tracking of the bead joined to the transducer. These experiments allow the measurement of parameters like dissociation rates and transition state parameters such as

https://doi.org/10.1017/S0033583522000075 Published online by Cambridge University Press

the distance to the energy barrier (Brampton *et al.*, 2011). Using BFP, several works have characterized the mechanical responses of different biomolecular interactions to external forces. For instance, Evans and coworkers used BFP to study the impact of pulling on cell surface bonds, such as how the pairing of P-selectin and PSGL-1 propagates and alters receptor-cytoskeletal linkage beneath the membrane. They described that PSGL-1 detaches from cytoskeleton prior to failure of the exterior adhesive P-selectin:PSGL-1 bond (Evans *et al.*, 2005; Evans and Kinoshita, 2007). Additionally, catch-slip behavior was identified for the interaction between PSGL-1 and P-selectin (Evans *et al.*, 2004). In another example, Perret and coworkers tested the homophilic interaction between E-cadherins molecules and opposing cells (Perret *et al.*, 2004). Furthermore, BFP has been used to study the intercellular adhesion molecule-1 (ICAM-1) with recombinantly activated $\alpha L\beta 2$ integrin by divalent cations (Evans *et al.*, 2010). BFP also allows quantifying how force and different conformations of lymphocyte function-associated antigen-1 regulate kinetics binding parameters with ICAM-1 (Chen *et al.*, 2010). See Fig. 1*b*.

Atomic force microscopy. AFM is a technique that works in a force range of 10–10^4 pN. It is unique in its ability to apply forces as high as nanonewtons. However, it is limited in its lower force resolution (lower than piconewtons) (Neuman and Nagy, 2008). The basic principle consists of coating both the tip of a microfabricated cantilever and a substrate surface with a low density of interacting molecules of interest (Robert *et al.*, 2007). The cantilever tip is brought to the surface of the substrate, so that the coated cantilever interacts with the substrate. This results in a mechanical force that will cause the cantilever to bend. Meanwhile, a laser beam that is reflected at the top of the cantilever is used to monitor the bending angle of the cantilever (Fuhrmann and Ros, 2010), which gives a measurement of force (Meyer and Amer, 1988). The measurement procedure consists of repeating cycles of approach and retraction at a constant speed on a given location. When the cantilever tip is pulled apart from the substrate surface, the force required for bond rupture can be recorded (Robert *et al.*, 2007). The frequency distribution of unbinding forces is obtained after enough cycles have been done (usually hundreds of approach–retraction cycles). Subsequent analysis of these rupture force values can be used to estimate the dissociation rate constants (Kada *et al.*, 2001; Lee and Marchant, 2001, 2003; Lo *et al.*, 2001; Zhang *et al.*, 2002; Cai and Yang, 2003; Kokkoli *et al.*, 2004; Kienberger *et al.*, 2005). Starting with the pioneering work on complementary DNA strands (Lee *et al.*, 1994*a*, 1994*b*), biotin–streptavidin (Florin *et al.*, 1994; Lee *et al.*, 1994*b*), and cell adhesion proteoglycans (Dammer *et al.*, 1995), this method has been applied to a wide range of interactions (Willemsen *et al.*, 2000): from complex biological intermolecular systems such as protein–nucleic acid (Bartels *et al.*, 2003, 2007; Kühner *et al.*, 2004; Baumgarth *et al.*, 2005; Fuhrmann *et al.*, 2009), antibody–antigen (Hinterdorfer *et al.*, 1996; Allen *et al.*, 1997; Morfill *et al.*, 2007), quadruplex nucleic acids (Lynch *et al.*, 2009), enzyme–inhibitor (Porter-Peden *et al.*, 2008), and cell adhesion molecules (Fritz *et al.*, 1998; Björnham and Schedin, 2009; Dague *et al.*, 2022) to supramolecular examples (Eckel *et al.*, 2005*a*) and synthetic biology (Eckel *et al.*, 2005*b*). See Fig. 1*c*.

Magnetic tweezers. MTs are a high-throughput method that can measure forces in the range of 10^{-3}–10^2 pN. MTs can manipulate superparamagnetic beads, with the external magnetic field from a pair of small permanent magnets placed above the sample holder of an inverted microscope. In these assays, receptor proteins are bound to the superparamagnetic beads and allowed to contact their surface-bound ligand. Then the permanent magnets above the trapping chamber produce a magnetic field gradient along the axial direction, resulting in a controlled force on the bead directed toward the magnets (Neuman and Nagy, 2008). MTs can be used to study several molecular interactions in parallel, offering an advantage *versus* other single-molecule force. For instance, this method has been used to study the prototypical ligand–receptor pair streptavidin–biotin (Claudia *et al.*, 2005; Shang and Lee, 2007; Kilinc *et al.*, 2012). See Fig. 1*d*. Finally, new experimental approaches have combined AFM with MTs (Muñoz *et al.*, 2015)

Acoustic force spectroscopy. AFS uses acoustic waves to apply controlled forces on microparticles in a flow cell. The exerted forces are in the range of sub-piconewtons to hundreds of piconewtons, with loading rates between 10^{-4} and 10^2 pN s^{-1} on thousands of protein–DNA complexes in parallel (Kamsma and Wuite, 2018). The flow cell consists of a piezo element and two glass layers with a fluidic channel in between. A protein–DNA complex attached by DNA end to a bead is allowed to contact the bottom glass coated with an interacting protein. The piezo element generates an acoustic wave that travels through the top glass to the bottom glass. The bottom glass reflects the acoustic wave, producing a standing wave over the flow cell. The bead exposed to this standing wave experiences a force along the vertical direction that applies tension to the interaction between the protein–DNA complex and the interacting protein (Lin *et al.*, 2018). See Fig. 1*f*. AFS can be used to study DNA–protein interactions like DNA–viral capsid protein assembly (Van Rosmalen *et al.*, 2020), DNA–RecA filament formation, and to determine the energy landscape of digoxigenin–antidigoxigenin bonds (Sitters *et al.*, 2014). Furthermore, AFS allows to probe the mechanical properties of cells (Sorkin *et al.*, 2018), the strength of molecular interactions of cells with the extracellular matrix (Kamsma *et al.*, 2018), and the unbinding behavior of carbohydrate binding modules to polysaccharide surfaces (Hackl *et al.*, 2021). See Fig. 1*f*.

Optical tweezers

OTs are based on the optical trapping phenomenon discovered in 1970 by Arthur Ashkin, for which he has recently been awarded the Nobel prize in 2018 (Nobel Prize, 2021). Optical trapping is achieved by tightly focusing lasers on a small volume (diameter on the order of micrometers) (Ashkin, 1970), where a nearby dielectric particle then experiences a restoring force toward the point of highest laser intensity. This keeps the particle stably confined in all directions, trapped at a single point. Forces in the range of 10^{-1}–10^2 pN can be exerted. These overlap with the range of forces experienced by biological molecules in their native environment; this makes OTs perfectly suited to study the forces between biomolecules (Neuman and Nagy, 2008). These complete reviews are recommended for instrumental details and technical information (Molloy and Padgett, 2002; Nieminen *et al.*, 2007; Zhang and Liu, 2008; Guo and Li 2013; Polimeno *et al.*, 2018; Zaltron *et al.*, 2020). OTs offer several advantages in the study of biomolecular interactions such as high spatio-temporal resolution, easy and specific attachment of biomolecules, and compatibility with fluorescent detection and visualization techniques such as Förster resonance energy transfer in hybrid custom-built (Comstock *et al.*, 2011; Whitley *et al.*, 2017) and commercial instruments (Avellaneda *et al.*, 2020). A notable example of

https://doi.org/10.1017/S0033583522000075 Published online by Cambridge University Press

commercial OTs are the miniTweezers instrument (Smith *et al.*, 2003), a compact single-optical trap capable of piconewton, sub-nanometric spatial-, millisecond temporal-resolution (see Fig. 1*e*).

Different experimental approaches have been developed to study intermolecular interactions using OTs. To discuss these experimental approaches, we will classify them into three groups: refolding and unfolding in *trans* interaction, constant force in *cis* interaction, and force ramp in *cis* interaction.

Detailed description of intermolecular interaction force experiments using OTs

To compare the experimental approaches mentioned above, we will discuss the difference between them in three experimental stages (see Table 1):

- Bead surface functionalization
- Real-time intermolecular interaction in OT
- Data analysis/processing

Bead surface functionalization

In this section, we describe the preparation to be done before the experiments. Specifically, the functionalization or derivatization of the beads and DNA handle.

Derivatization of the beads

A critical preliminary step is the binding of the relevant molecules to the beads (the order of magnitude of the diameter from $\sim 10^1$ nm to 10^1 μm; Neuman and Nagy, 2008). There are many experimental approaches to attach molecules to beads, and a variety of beads to use (see Fig. 2*b*). Although polystyrene beads are the most common (Ramírez *et al.*, 2017; Burgos-Bravo *et al.*, 2018), latex (Mejean *et al.*, 2009), silica (Block *et al.*, 1990), and germanium (Sudhakar *et al.*, 2021) beads are also available. There are several types of beads with different kinds of functionalization that can be used depending on the molecule to be studied: Ni-NTA-coated beads can be used to directly bind his-tagged proteins (Mejean *et al.*, 2009); G-protein-coated beads can be utilized to bind the molecule of interest through Fc-fusion proteins (Burgos-Bravo *et al.*, 2018), specific antibodies (Peña-Oyarzun *et al.*, 2020), or by modified-DNA linkers called 'DNA handles' (Ramírez *et al.*, 2017); streptavidin- or neutravidin-coated beads can also be used to bind the molecule directly (e.g. a biotinylated-protein) or through a biotinylated-DNA handle. G-protein- and streptavidin-coated beads are the most commonly used in OTs as they form strong bonds and are commercially available. The derivatization strategies of these polystyrene beads will be described below.

Protein G-coated polystyrene bead/primary antibody against protein of interest. For proteins, protein G-coated beads can directly bind a fusion protein containing an IgG-Fc tag (Burgos-Bravo *et al.*, 2018). A primary antibody against the protein of interest can be used in combination with protein G (Peña-Oyarzun *et al.*, 2020; Mateluna *et al.*, 2022). For this option, protein G-coated beads are incubated with a primary antibody that binds the protein to be immobilized on the bead. Then, a crosslinking agent is used to covalently bind the protein G and the Fc tag or antibody (Peña-Oyarzun *et al.*, 2020).

Protein G- or streptavidin-coated polystyrene beads/DNA handles. Another possibility to attach the protein of interest to polystyrene beads is using DNA handles (Ramírez *et al.*, 2017). This approach can be used for studying interactions between proteins (Ramírez *et al.*, 2017) and non-protein molecules like aptamers (Casanova-Morales *et al.*, 2019). DNA handles are constructs between 500 and 1500 bp (Cecconi *et al.*, 2008; Kaiser *et al.*, 2011) that act as linkers between the protein and the bead (Halvorsen *et al.*, 2011). These constructs separate the protein from the optically trapped bead, eliminating undesired interactions and photodamage. Shorter DNA handles (e.g. 29 bp) can be used to enhance the signal to noise ratio (Forns *et al.*, 2011).

A DNA–protein complex is typically formed through a disulfide bond between a cysteine residue on the protein of interest and a cysteine at one end of the DNA handle (Ramírez *et al.*, 2017). Enzyme-based coupling strategies have also been used to form a covalent protein–DNA handle bond, including HaloTag fusion proteins that perform a dehalogenase reaction with the HaloTag ligand cross-linked to DNA handle (Aubin-Tam *et al.*, 2011). By polymerase chain reaction (PCR), DNA handles are made using digoxigenin or biotin moiety-functionalized primers (Cecconi *et al.*, 2011). The process allows the binding of the DNA–protein complex to the protein G-coated spheres that have been derivatized with anti-digoxigenin (anti-dig) antibodies or streptavidin beads. The protein G or protein G/primary antibody methodology described above can also be used for refolding–unfolding and force–ramp experiments (Bustamante *et al.*, 2017).

The derivatization strategy to be used depends on the molecules that will be studied. When using DNA handles, at least 40% of the cysteine residue in a protein needs to be exposed to the solvent (Wilson, 2011), and at the opposite side of the interaction. If an intrinsic cysteine residue is not available, a mutant protein can be fabricated by replacing a serine residue with cysteine (Ramírez *et al.*, 2017). However, the retention of the native protein conformation must be confirmed. If there is a cysteine (wildtype or mutant) that meets these requirements, then the use of DNA handles is appropriate. When working with other molecules such as aptamers, the DNA handle approach can be appropriate, but there must be an SH moiety in order to bind the handle. In the case of aptamers, they can be directly bound to the DNA handles by their 3′ and 5′ ends (Cecconi *et al.*, 2008). The DNA handle approach can be utilized on refolding and unfolding in *trans* interaction and constant force in *cis* interaction. For refolding and unfolding in *trans* interaction, there need to be two cysteine residues on the same molecule and at opposite sides. On the other hand, the protein G and protein G/primary antibody method requires the availability of a specific antibody that binds the molecule on the opposite side of the interaction. Nevertheless, a chimera of the target protein can be synthetized, for instance by adding a GFP protein (Thoumine *et al.*, 2008), GSH molecule (Nicholas *et al.*, 2014), or Fc tag (Burgos-Bravo *et al.*, 2018). Fusion proteins allow working with non-purified protein extract because of the binding specificity (Burgos-Bravo *et al.*, 2018). Large molecules might be directly attached to spheres, while DNA handles are recommended for small molecules since surface imperfections on the polystyrene beads are always present at the Angstrom level. Thus, DNA handles avoid the possible interference of the bead surface when the size of the molecule is smaller than the imperfections of the polystyrene beads. The DNA handles function as spacers between the protein and the beads, keeping interactions between the tethering surfaces to a minimum (Cecconi *et al.*, 2011) and preventing photodamage of the protein of interest (Chen *et al.*, 2019; Desai *et al.*,

https://doi.org/10.1017/S0033583522000075 Published online by Cambridge University Press

https://doi.org/10.1017/S0033583522000075 Published online by Cambridge University Press

Table 1. Detailed description of intermolecular interaction force experiments using OTs

Name		Refolding and unfolding in *trans* interaction		Constant force in *cis* interaction	Force ramp in *cis* interaction
General description		One protein is trapped between the beads and the other is in solution		Each protein is trapped in each bead and a force jump is applied, waiting until interaction breaks.	Each protein is trapped in each bead and a force ramp is applied until the interaction breaks.
Bead surface functionalization		It depends on the type of molecules and interactions to be studied; molecules are either attached directly to the beads or through handles.			
		OT experimental step description.			
Real-time intermolecular interaction in OT	Sample preparation	Molecules are first diluted to single-molecule concentration and then connected to the beads.			
	Functionalized beads catching	Beads containing the molecules of interest are optically trapped in each microchannel of the flow chamber, and the setup for the study of interaction between the molecules is prepared.			
	OT experiment	Once the molecule is tethered between the beads, it is stretched by pulling at constant velocity until it unfolds, and then is gradually relaxed until the molecule is refolded. The unfolding and refolding cycle is repeated to observe the frequency of unfolding/refolding signatures (i.e. rip and zip).		Once the interaction is observed (by the increase in force) force is quickly set and sustained at a constant level until the bond is broken. The lifetime (τ) of interaction is measured directly from the measurement.	Beads are approached to promote the interaction between the molecules, then the beads are pulled apart at a constant loading rate until the bond is broken. This approach–separation cycle is repeated several times to collect rupture forces.
Data analysis/ processing	Analysis	Experimental data	Lifetime of interaction histogram. Rip force probability, time intervals that the protein remained bound and unbound are obtained. Their histograms or averages are calculated. Rips probabilities are characterized.	Interaction lifetime histograms at different forces.	Force ramp in *cis* interaction histogram to molecule interaction. Force ramp in *cis* interaction histogram to non-specific interactions. Rupture force histograms for both specific and non-specific interactions are prepared.
		Thermodynamic and kinetic constants	K_D, k_{off}, k_{on}	The lifetime of the interaction at the constant force. It is adjusted by the DHS model to obtain energy to the transition state $\Delta G^{\neq}$, distance to the transition state $\Delta x^{\neq}$.	Rupture force histograms without non-specific interactions. Lifetime of interaction τ is calculated and by fitting to DHS model, one can obtain energy to the transition state $\Delta G^{\neq}$, distance to the transition state $\Delta x^{\neq}$.

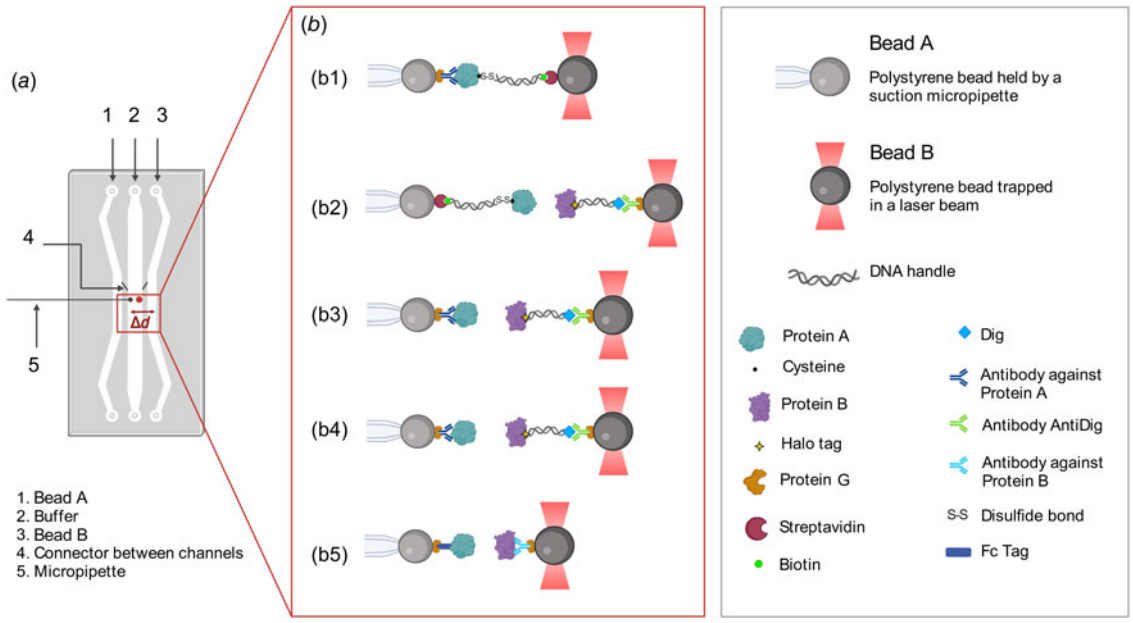


Fig. 2. Bead experimental setup with miniTweezers. (*a*) Laminar flow chamber used in miniTweezer setup: two microchannels (1 and 3) are connected to the main channel (2) by connectors (4). Channels 1 and 3 allow the controlled entry of the functionalized beads with the proteins of interest. Bead A is injected by channel 1 and at the main channel is trapped and guided with the optical trap to a suction micropipette (5). Functionalized bead B enters by channel 2, at the main channel is trapped and guided with the optical trap in front of bead A. (*b*) Five examples of construct combinations that can be studied in OT. (b1) Bead A/Protein_G/anti_protein_A ↔ protein_A/cystein/S-S/DNA_handle/biotin/streptavidin/bead B. (b2) Bead A/streptavidin/biotin/DNA_handle/S-S/cysteine/Protein_A ↔ Protein_B/Halo_tag/DNA_handle/Dig/Anti_Dig/ProteinG. (b3) Bead A/proteinG/anti_protein_A/Protein_A ↔ Protein_B/Halo_ta/DNA_handle/Dig/Anti_Dig/ProteinG. (b4) Bead A/anti_protein_A/Protein_A ↔ Protein_B/Halo_ta/DNA_handle/Dig/Anti_Dig/Protein_G. (b5) Bead A/Protein_G/Fc tag/Protein_A ↔ Protein_B/Anti_proteinB/Protein_G. (*c*) Box with names of molecules involved.

2019). In this way, DNA handles minimize thermal and acoustic fluctuations, which is especially useful when there are impurities within the sample (Halvorsen *et al.*, 2011). These derivatization strategies can be combined in the final experimental setup. For example, DNA handles and the protein G or protein G/primary antibody approaches can be used to bind each of the molecules of study. Therefore, when choosing a strategy for binding the molecule of interest to the bead, all the factors mentioned above must be taken into consideration.

Real-time intermolecular interaction in OTs

Preparing samples for OTs

As previously mentioned, the preparation of the samples is slightly different when using protein G/primary antibody *versus* DNA handles. In the case of protein G/primary antibody, the derivatization is performed in advance, and the binding of the protein to the beads occurs immediately before the experiment. In contrast, for DNA handles, the bead derivatization process is the first step (e.g. with anti-dig) followed by DNA handle-target molecule construct preparation (Fig. 2*b*). The complex is then incubated with the beads immediately before the experiment. A brief description of these two strategies will be given.

Preparation of the protein G-coated bead/primary antibody/protein complex. The derivatization of the beads is made as previously explained. After derivatization, a passivation process is recommended to prevent unwanted interactions. The passivation is carried out by incubating the beads with 1% w/v bovine serum albumin diluted in the interaction buffer (the buffer that will be used for the OT experiments) for 4 h at room temperature, then washing in the same buffer by centrifugation (Szili *et al.*, 2012). Passivation can also be done by adding β-casein at a final concentration of 1 mg ml^{-1} followed by incubation while vortexing for 1 h at room temperature (Fukuda *et al.*, 2020). After passivation, the beads can be stored at 4 °C in the presence of sodium azide (0.05% w/v) for up to a year. To form the complex with the protein, the beads (0.5%, w/v) are incubated at the nanomolar concentration on ice or room temperature for 15 min. Then the beads are ready to be injected into the microfluidic chamber of the OTs (Fig. 2*a*).

Preparation of the streptavidin-coated bead/DNA handle/protein complex and protein G-coated bead/anti-dig antibody/DNA handle/protein complex. The first step is to synthesize the DNA handles (Cecconi *et al.*, 2008). The handles are synthesized via PCR in a thermal cycler using a plasmid or lambda DNA and appropriately functionalized primers (Cecconi *et al.*, 2008). For synthesizing biotin-DNA-SH handles, one of the primers contains a biotin moiety and the other contains an SH moiety, so the result will be DNA handles with a biotin and an SH group at each end. In the case of digoxigenin- DNA-SH handles, one primer contains a digoxigenin moiety instead of the biotin-primer. Primers with two dig moieties can also be used in order to guarantee more stability in the binding between the molecule and DNA handle (Desai *et al.*, 2019). The biotin or digoxigenin-DNA molecules are then bound to the streptavidin or anti-dig-coated beads, respectively. Then, the DNA handle-molecule construct can be made via disulfide bonding formation (Wilson, 2011).

The microfluidic channels of the OT setup are filled with buffer solution before injecting the derivatized beads as described in the following section.

https://doi.org/10.1017/S0033583522000075 Published online by Cambridge University Press

Trapping functionalized beads

In this step, the beads functionalized with the molecules of interest are trapped and brought in contact to promote the protein–protein interaction. The laminar flow microfluidic chamber has three independent channels with small glass tube interconnections, physically separating the two different types of beads (Fig. 2*a*). The central channel has a micropipette connected to the outside of the microfluidic chamber. The catching process corresponds to trapping the beads from the different channels of the microfluidic chamber and bringing them to the central channel of the chamber where the experiment is carried out. The procedure for an experiment is as follows:

(1) The functionalized beads are injected into the upper and lower channels.
(2) A dual-laser (808 or 845 nm) optical-trap (trap stiffness of 0.1 pN nm^{-1}) is used to trap the bead in one of the channels and move it to the central channels where the micropipette is.
(3) Suction is applied on the micropipette to hold one of the beads in place.
(4) The optical trap is used to bring the second bead from the other channel close to the micropipette-trapped bead.
(5) The beads are briefly brought into contact (less than ∼3 s) to promote interaction between the molecules.

OT experiment

Once the interaction is formed, tension is applied on the construct in order to measure its physical properties. As mentioned above, there are three main ways to measure interactions using OTs (Table 1):

- Refolding and unfolding in *trans* interaction (one protein is trapped between the beads and the other is in solution).
- Constant force in *cis* interaction (each protein is trapped in each bead and a force jump is applied waiting for the interaction to break).
- Force ramp in *cis* interaction (each protein is trapped in each bead and a force ramp is applied until the interaction breaks).

Refolding and unfolding in trans *interaction*

This experimental approach consists of repeated cycles to mechanically pull a molecule until it loses its natural structure and then lower the tension until the molecule refolds. The beads are brought into contact for ∼1 s or less (step 5 in Section 'Trapping functionalized beads'). Then, the optical trap is moved away at a constant speed (order of magnitude ∼10–100 nm s^{-1}) (Bustamante and Smith, 2007) from the bead that is fixed in the pipette. If the molecules bond successfully while the beads are in contact, the extension–force curve will be with a positive slope (Fig. 3*a*), otherwise, the slope is null and the beads should be brought back into contact. As the optical trap is moved away, a sharp drop (or 'rip') in the tension can be observed whenever a specific structure of the molecule of interest unfolds. Finally, after completely unfolding the molecule, the optical trap is returned to its initial position, causing the system to relax and letting the molecule fold again. The experiment is repeated in the presence or absence of an interacting protein or other molecule added in *trans* in the buffer, and the frequency of rips is observed. These data are displayed as rip force histograms, from which the lifetime histogram is obtained.

For example, the in *trans* interaction scheme was used to study the interaction of binding immunoglobulin protein (BiP), a major chaperone from the endoplasmic reticulum, with its protein substrate, the MJ0366 (Ramírez *et al.*, 2017). Here, BiP was added in *trans*, while the MJ0366 protein was tethered between two beads (Fig. 3*a*). Since BiP interacts with unfolded proteins (Schmid *et al.*, 1994), OTs were used to mechanically control the folded state of the substrate. The MJ0366 protein was unfolded by pulling the optically trapped bead at a constant loading rate and refolded by lowering the tension (i.e. relaxing cycle). Experiments performed in the presence of BiP showed a loss of refolding and unfolding events in the consecutive pulling–relaxing cycles (Fig. 3*a*) in contrast to the experiments in the absence of BiP, verifying that BiP binds to the unfolded state of MJ0366 protein and prevents its refolding. From these features in the force–extension curves, the BiP's dissociation constants were calculated by measuring the probabilities for observing rips (the presence of unfolding and refolding events) and no rips (the absence of unfolding and refolding events). The reversibility of BiP binding to its substrate was also determined due to the reappearance of refolding and unfolding events. The time intervals that BiP stayed bound (e.g. disappearance of unfolding/refolding events, τ_{off}) or unbound (e.g. reappearance of unfolding/refolding events, τ_{on}) to the protein substrate were directly calculated. The corresponding k_{off} and k_{on} were estimated by assuming an exponential distribution for the off and on lifetimes (Ramírez *et al.*, 2017). It was also determined that the binding–unbinding of BiP to its substrate depends on both the type and concentration of nucleotide, indicating that ATP hydrolysis regulates the binding and release of this chaperone to the substrate protein (Ramírez *et al.*, 2017).

Naturally, this assay can be used to study the binding between other kinds of molecules. For example, a refolding and unfolding experiment was used to study the dynamics of APTSTX1–aptamer, a single-stranded DNA molecule with a high affinity for saxitoxin (STX), a lethal neurotoxin (Casanova-Morales *et al.*, 2019).

Constant force in cis *interaction*

Constant-force assays (also called force-clamp assays in the literature) have been widely used to study protein interactions. In this assay, the beads are brought into contact for ∼2 s or less in order to promote the interaction between the proteins (step 5 in Section 'Trapping functionalized beads'). Once the binding is confirmed by an increase in the tension, the optical trap is fixed at a constant force. The duration of the interaction is measured, until the bond rupture is observed as a sudden decrease in the tension. This time is related to the lifetime τ of the interaction at a specific force. Then, the experiment is repeated in order to measure the decay times as a function of the force. This strategy should be repeated a minimum of 20 times, and at least five pairs of new beads should be used for each measured force.

The range of forces that will be applied to the molecule depends on previous information and characteristics of the interaction. If this is unknown, a large range of forces can be used initially to find the most relevant region for a given interaction. It is recommended to complement the experiment with the previous force ramp experiment, which can also provide some information on τ at different forces. Using these data, it is possible to extract kinetic parameters by using the Dudko–Hummer–Szabo (DHS) model (Dudko, 2008).

For instance, the dynamic-catch bond behavior was described for the first time in the characterization of the interaction of

https://doi.org/10.1017/S0033583522000075 Published online by Cambridge University Press

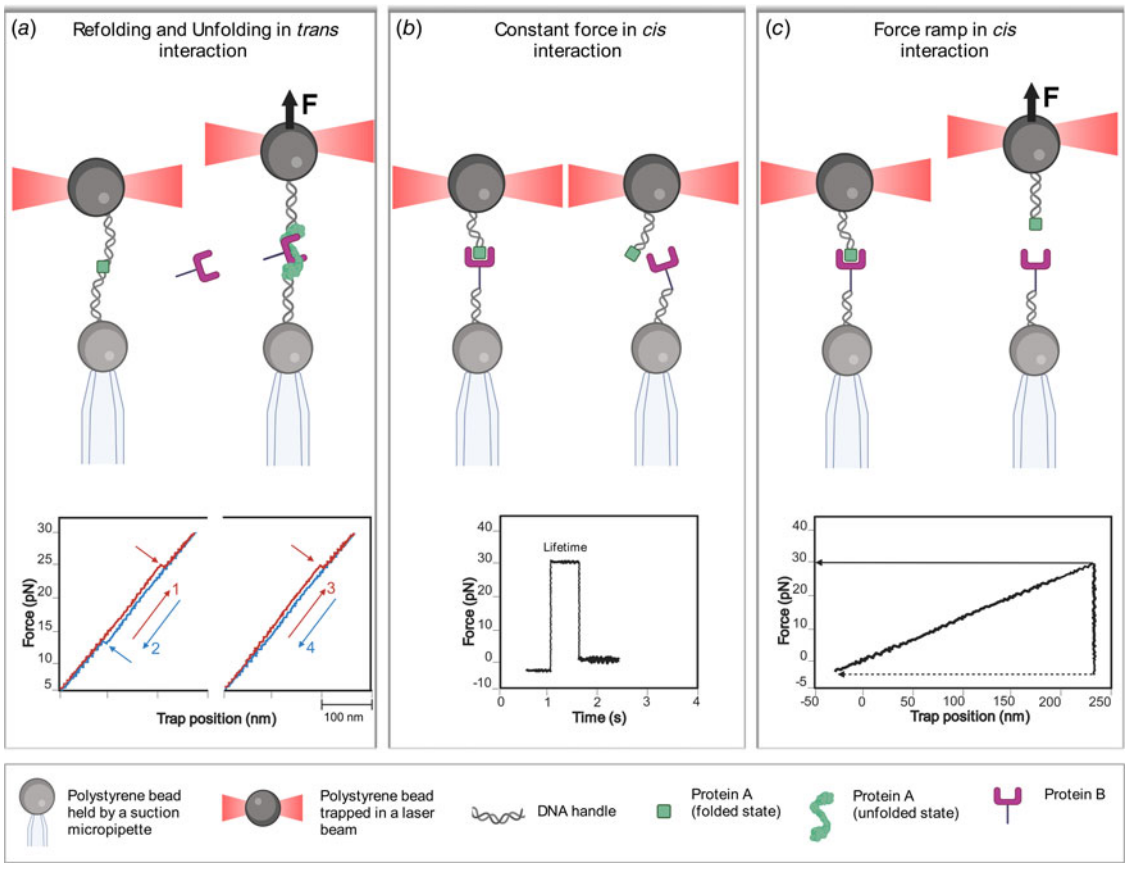


Fig. 3. Intermolecular interaction force experiments using OT. (*a*) Refolding and unfolding in *trans* interaction: at the top, protein A (green square) is tethered between two dsDNA handles attached to a bead held by a suction micropipette and an optically trapped bead. The optically trapped bead is pulled apart at a constant loading rate (arrow direction) stretching the molecule until it unfolds. Then protein B (purple) is added to the buffer and binds to the unfolded state of protein A preventing its refolding. At the left bottom, force–extension curves of the mechanical folding and unfolding events. The unfolding cycles are shown in red, and relaxation traces with refolding events at lower forces are shown in blue. The panel to the right shows no refolding event due to the binding of the interacting partner to the unfolded state. (*b*) Constant force in *cis* interaction: at the top, beads are approached to promote the interaction between the proteins. Once the interaction is observed, force is set and sustained constant until the bond is broken. At the bottom is a force–time graph. The interaction event is observed as an increase in the axis of force. The lifetime of the interaction is obtained directly from the graph corresponding to the time between the force is set and sustained constant until the bond is broken, observed as a sudden drop in force. (*c*) Force ramp in *cis* interaction. At the top, beads are approach and brought into contact to promote the interaction between the proteins. Then beads are separated by pulling apart the optically trapped bead at a constant loading rate (arrow direction) until the bond is broken. At the bottom is a force–extension curve. In case of interaction, an increase in the axis of force is noticed. Then at a certain distance the rupture of the interaction is produced, observed as a sudden drop in force.

Thy-1 with both $\alpha_5\beta_1$ integrin and syndecan-4 by BFP (Fiore *et al.*, 2014). Other constant-force assays include F-actin and G-actin dissociation kinetics (Lee *et al.*, 2013), kinetochore-microtubule attachments (Akiyoshi *et al.*, 2010), P-selectin, and PSGL-1 binding (Marshall *et al.*, 2003).

On- and off-rates, mechanical stability and affinity measurements have been measured by studying proteins directly attached to the surface of the beads (Fig. 2*b*). For instance, the specific interactions between glycosylphosphatidylinositol-anchored Thy-1 protein, an abundant neuronal cell adhesion molecule, and its astrocytic receptors, the transmembrane $\alpha_v\beta_3$ integrin and the proteoglycan of heparan sulfate syndecan-4, was characterized using this approach (Burgos-Bravo *et al.*, 2020). For this, Fc-tagged recombinant molecules were used to allow direct coupling to the beads via the strong and high-affinity Fc-protein G interactions (Fig. 2*b*). Specifically, the bond lifetime of the Thy-1-dependent interaction as tri-molecular complex (i.e. Thy-1-Fc/syndecan-4-Fc + $\alpha_v\beta_3$-Fc) was determined by constant-force assays (Fig. 3*b*), where the duration before bond dissociation is measured directly under different forces. The force-dependent lifetime data were fitted using the Bell (1978) model showing an ordinary slip-bond behavior for the tri-molecular complex (Burgos-Bravo *et al.*, 2020). Furthermore, the Bell model was also used to calculate the kinetic parameters of the unbinding process, obtaining a k_{off} at zero force of ~0.08 s^{-1} and distance to the transition state of ~0.2 nm.

Force ramp in cis *interaction*

Another strategy to study molecular bonds are force-ramp assays. In this approach, the forces required for bond dissociation (i.e. rupture forces) are measured and used to obtain force-dependent kinetic parameters and mechanical response of molecular bonds. Rupture-force data are obtained by pulling apart the optically trapped bead at a constant loading rate after the beads are brought into contact and then an interaction is formed (also referred to as approaching and retraction cycle; see detailed explanation in Section 'Detailed description of intermolecular interaction force experiments using OTs'). As shown in Fig. 3*c*, rupture force values resulting from single-molecule bindings are determined directly from the force–trap position traces with a single-step bond

https://doi.org/10.1017/S0033583522000075 Published online by Cambridge University Press

rupture signature (Litvinov *et al.*, 2005). The beads are brought into contact to promote protein–protein interaction (step 5 in Section 'Trapping functionalized beads'). Then the optical trap is pulled apart at a constant velocity, much like in folding/unfolding experiments. The interaction between the two molecules resists the pulling, generating a measurable tension that increases with distance. After enough force is applied, the interaction yields, and the tension force drops suddenly to zero. The maximum force achieved before the separation of the system is then recorded as the 'rupture force' (Fig. 3*c*). These approach–tension–release cycles are repeated at least 50 times for an average pair of beads. Beads are changed approximately six times in order to achieve around 300 total pulling events, with and without interaction (a number easily achievable in a single-productive day and can be sufficient for robust statistics). These data are displayed as force ramp histograms, for which the underlying probability distribution can be fitted in order to extract the kinetic parameters.

Force-ramp assays were used to obtain rupture force data for the Thy-1/$\alpha_v\beta_3$ integrin interaction (Burgos-Bravo *et al.*, 2018). In this study, the most probable bond rupture force or bond strength of ∼25 pN was determined pulling at a constant loading rate of 10 pN s^{-1} (Burgos-Bravo *et al.*, 2018). The force magnitude was in the previously reported range for non-covalent interactions (Weisel, 2003). Likewise, bond strengths between 25 and 44 pN were reported for the interactions between *Staphylococcus aureus* protein A and several species immunoglobulin G molecules, such as rabbit and goat, by using OT and force-ramp assays (Stout, 2001). The kinetic parameters of the force-induced dissociation process can be characterized using the DHS model (Eq. (9); Dudko *et al.*, 2008), which permits transforming the rupture force histograms into force-dependent lifetimes $\tau(F)$ (for more details see Section 'Detailed description of intermolecular interaction force experiments using OTs'). This methodology permitted the characterization of the complete energy landscape ($\Delta x^{\ddagger} \sim 0.50$ nm and $\Delta G^{\ddagger} \sim 5.54 k_B T$) and the zero-force kinetic parameter ($k_{off}{}^{0} \sim 0.051\ s^{-1}$) of the Thy-1/$\alpha_v\beta_3$ dissociation process (Burgos-Bravo *et al.*, 2018). Moreover, the force-dependent lifetime showed that force exponentially increased Thy-1/$\alpha_v\beta_3$ integrin dissociation, indicating a slip-bond behavior for this molecular bond.

Applying the single-molecule OT technique, the binding specificity and direct interaction between a pair of proteins can be determined from the frequency of adhesion measurements (e.g. the probability for adhesion based on the total number of contacts) (Robert *et al.*, 2007; Stangner *et al.*, 2013). Events with and without binding are used to calculate adhesion frequency in a sequence of approaching–retraction cycles between both beads during the force-ramp experiments. This strategy was used to verify the specific interaction between syndecan-4 and Thy-1 (Burgos-Bravo *et al.*, 2020). Using a similar strategy, Peña-Oyarzun and coworkers confirmed the existence of a protein complex between the mechanosensory Ca^{2+} channel polycystin 2 (PKD2) and scaffolding protein Beclin 1 (BECN1), two autophagy-related proteins (Peña-Oyarzun *et al.*, 2020). Here, to perform OT experiments, GST-PKD2 and 6xHis-BECN1 fusion proteins were attached to GSH- and anti-His-coated polystyrene beads, respectively. A bond strength of ∼12 pN average (loading rate of 10 pN s^{-1}) and a dissociation rate of ∼0.28 s^{-1} were calculated for the PKD2/BECN1 protein complex, suggesting a weak and transient protein–protein interaction. Moreover, an ordinary slip-bond behavior was described for this complex. By using this technique, a physical interaction was identified between PKD2 and BECN1 that is required for autophagosome formation in human cells. Recently, this strategy has been used to prove the interaction between histatin-1 and the receptor VEGFR2 (Mateluna *et al.*, 2022). Based on the kinetic parameters and rupture forces obtained, the authors proposed that the histatin-1–VEGFR2 interaction is specific but transient.

A tether ligand assay is another strategy that can be used to measure binding rates of ligand–receptor pairs under force. Here, the goal is to hold the same binding partners in spatial proximity under mechanical control. A fusion construct is prepared between a pair of interacting proteins joined by a flexible polypeptide linker. This allows the measurement of repeated interactions of the same pair of molecules. This strategy has provided insights into von Willebrand factor (VWF) binding of the glycoprotein Ibα subunit (GPIbα) on the surface of platelets (Kim *et al.*, 2010, 2015), its essential role in the platelet plug formation, and their resistance to strong hydrodynamic forces. A complex was formed between GPIbα and the A1 domain of VWF using a polypeptide linker and attached to a pair of beads by DNA handles. By moving the optically trapped bead, this construct was subjected to pulling and relaxing cycles (e.g. force-ramp assay), allowing the unbinding and rebinding of the GPIbα–A1 complex. Both unbinding and binding processes are characterized by the abrupt increase and decrease in the tether length, respectively. This experimental strategy has also been used to study the force-sensitive mechanosensory role of filamin (Rognoni *et al.*, 2012).

Both force-ramp and constant-force assays have been extensively used to study the mechanical regulation of molecular interactions by experimentally measuring kinetic parameters under force. However, some differences have been described for both strategies. The force-ramp gives a higher throughput than constant-force assays. In the first strategy, the rupture forces are obtained from all binding events, while the constant force measures the lifetime from a fraction of binding events that survive the jump into the desired force. The bond lifetime values are obtained directly by the constant-force approach, without the extra data processing/analysis needed in force-ramp experiments. Moreover, when force is ramped at a constant rate, the rupture forces are measured in a dynamic condition. In contrast, when the force is clamped at a constant level, the bond dissociation is determined under static conditions, where the same force is applied to all components in the system, including interacting molecules, force sensor, and molecular linkers. Interestingly, using the constant force setup, it was possible to discover the catch (Marshall *et al.*, 2003) and ideal bonds (Rakshit *et al.*, 2012).

Considering the high sensitivity of this single-molecule technique, purified proteins are desirable to study unbinding parameters using OTs, for example, to reduce the rupture force resulting from non-specific interactions. The strength estimated for these non-specific binding events can reach values of ∼10 pN (Weisel, 2003). Even when this rupture force peak might differ from the obtained for the specific dissociation between the proteins of interest, the non-specific interaction distribution partly overlaps with the lower rupture forces range produced by specific protein–protein interactions. To address this issue, a novel mathematical approach based on the law of total probabilities was designed to effectively correct the rupture force measurements for non-specific binding events, consequently obtaining an accurate estimation of the specific rupture forces for protein–protein dissociation and calculating the kinetic and transition state parameters (Burgos-Bravo *et al.*, 2018). A complete description

https://doi.org/10.1017/S0033583522000075 Published online by Cambridge University Press

of the mathematical correction is given in Section 'Detailed description of intermolecular interaction force experiments using OTs'. It has been reported that the work with purified protein still suffered from residual non-specific interactions (Burgos-Bravo *et al.*, 2018), highlighting the importance of this mathematical correction method when single-molecule protein–protein interaction studies are performed.

Data analysis/processing

We will detail the strategies to analyze the data for the three experiments mentioned above:

- Refolding and unfolding in *trans* interaction strategy. It is possible to obtain the dissociation constant K_D, and kinetics constants (k_{off}, k_{on}).
- Constant force in *cis* interaction strategy. The lifetime of the interaction at the constant force. It is adjusted by the DHS model to obtain energy to the transition state $\Delta G^{\neq}$, and distance to the transition state $\Delta x^{\neq}$.
- Force ramp in *cis* interaction strategy. Rupture force histogram without non-specific interactions. Lifetime of interaction τ are calculated. By fitting to the DHS model, one can obtain the energy to the transition state $\Delta G^{\neq}$, and distance to the transition state $\Delta x^{\neq}$.

Refolding and unfolding in trans interaction strategy

It is possible to calculate the dissociation constant K_D of molecule for the used substrate (Ramírez, 2016):

$$K_D = \frac{[S]\ [\text{Molecule}]}{[S{:}\text{Molecule}]} = [\text{Molecule}]\frac{P_{rip}}{P_{nrip}} = [\text{Molecule}]\frac{P_{rip}}{1-P_{rip}} \quad (1)$$

where $[S]$ is the concentration of the substrate molecule, [Molecule] is the concentration of the molecule, [*S*:Molecule] is the concentration of the molecule–substrate complex, and P_{rip} and P_{nrip} are the probabilities for observing rips and no rips.

The time intervals that the molecule stay bound and unbound to the substrate can be determined directly, and the corresponding on and off rates can be calculated. By assuming a first-order reaction for the on and off times, the on and off rate constants can be calculated from the inverse average of the on and off times:

$$-\frac{d[A]}{dt} = k[A] \quad (2)$$

$$[A] = [A]_0 e^{-kt} \quad (3)$$

A first-order reaction, which is modeled by an exponential distribution for the on and off times, proceeds at a rate linearly dependent on only one reactant concentration, represented by *A*, where *k* is the rate constant and *t* is the residence (or absence) time.

The mean for the probability density to the k_{off} at absence time (*at*) and k_{on} at residence time (*rt*) are:

$$\text{mean}(at) = \frac{1}{k_{off}} \quad (4)$$

$$\text{mean}(rt) = \frac{1}{k_{on}} \quad (5)$$

The K_D can also be calculated using these parameters:

$$K_D = \frac{k_{off}}{k_{on}} \quad (6)$$

Constant force in cis interaction strategy

For interpreting this force dependence of the lifetime, the $\tau(F)$ data can be fitted by the prediction of the DHS model. This model predicts the force-dependence of the lifetime assuming that the dissociation of protein–protein binding can be described as an escape from a one-dimensional free energy well (Dudko *et al.*, 2008). Therefore, by fitting to the non-linear DHS model, the energy landscape and kinetic parameters of the dissociation process at a constant loading rate can be obtained.

Obtaining biochemical parameters through the DHS model

Once the specific force histogram is obtained, it is normalized and fitted to the DHS model (Dudko *et al.*, 2008). First, it is necessary to calculate the lifetimes of the interaction with force dependence, $\tau(F)$:

$$\tau\left(F_0 + \left[k - \frac{1}{2}\right]\Delta F\right) = \frac{\left(h_k/2 + \sum_{i=k+1}^{N} h_i\right)\Delta F}{h_k \dot{F}(F_0 + [k-1/2]\Delta F} \quad (7)$$

In this equation, k is an integer, with values 1, 2,…, $N-1$, N indicates the number of a bar on the histogram. F_0 is the minimum recorded force, and ΔF is the width of the bars of the histogram. Each bar has a height h_k, corresponding to the counts in bar k, C_k, normalized so that the total area is equal to: $h_k = C_k/C_{Tot} \cdot \Delta F$, with C_{Tot} being the total number of accounts. The loading rate $\dot{F}$ is the rate of change in force over time. When modeling the DNA handles as a worm-like chain, the loading rate corresponds to:

$$\dot{F}(F) = v\left[\frac{1}{k_s} + \frac{2\beta L_C L_P(1+\beta F L_P)}{3+5\beta F L_P + 8(\beta F L_P)^{5/2}}\right]^{-1} \quad (8)$$

where v is the constant speed of the experiment (in our case 100 nm s^{-1}). The spring constant of the miniTweezers, k_s, has a value of 0.1 pN nm^{-1}. The contour length (L_C) is the end-to-end length of the DNA handle, in this case 180 nm. The persistence length, (L_P) (Bouchiat *et al.*, 1999), is the characteristic length at which the chain remains rigid. In the case of double-stranded DNA, L_P has an average value that depends on the experimental conditions. In physiological buffer, it is ~50 nm (Bustamante *et al.*, 2003). $\beta = (k_B T)^{-1}$ corresponds to the reciprocal of the thermal energy.

Then, the lifetimes of the interaction in dependence on force are given by:

$$\tau(F) = \tau_0\left(1 - \frac{\nu F \Delta x^{\neq}}{\Delta G^{\neq}}\right)^{1-1/\nu} e^{-\beta\Delta G^{\neq}[1-(1-\nu F\Delta x^{\neq}/\Delta G^{\neq})^{1/\nu}]} \quad (9)$$

From the previous expression, at zero force, three parameters are obtained:

https://doi.org/10.1017/S0033583522000075 Published online by Cambridge University Press

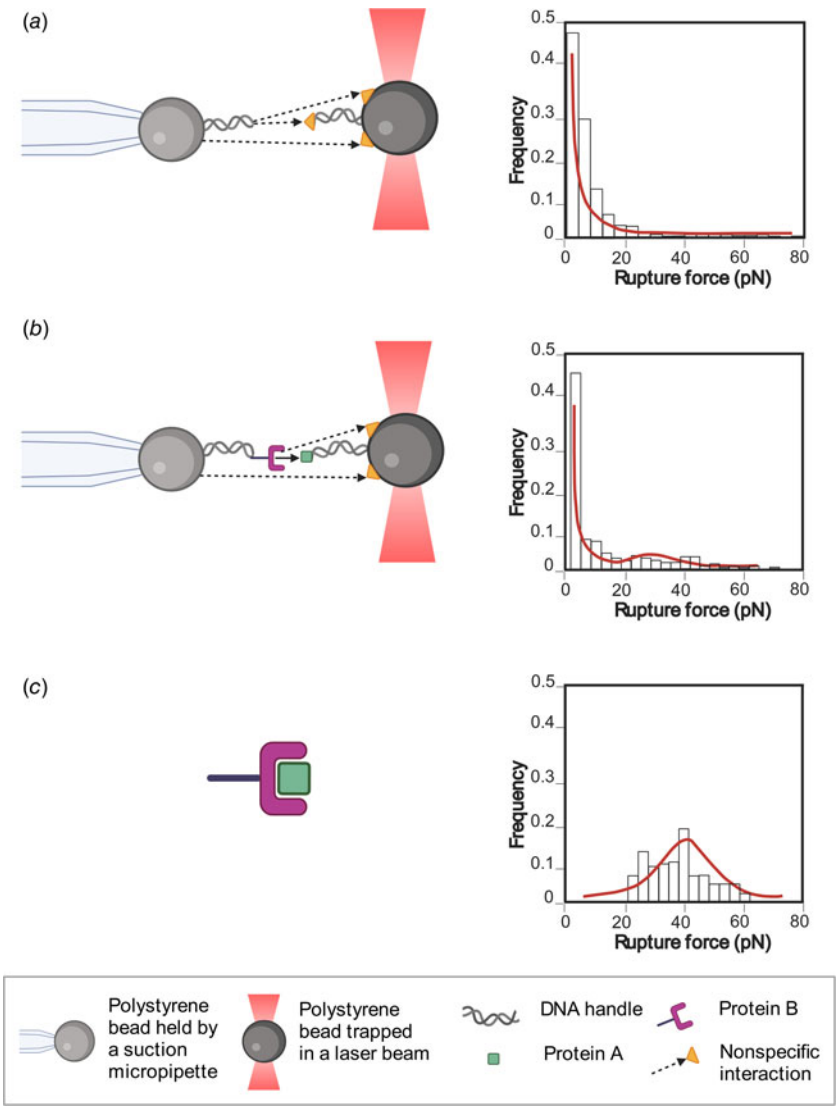


Fig. 4. Methodology to obtain the specific interaction forces between the molecules of interest. The illustration shows the interactions of the molecules and their respective histograms. (*a*) Control histogram: the forces of non-specific interactions, represented by a yellow triangle and dashed black arrows, are measured using the components of the construct without the proteins of interest (proteins A and B), resulting in a force histogram of non-specific interactions. (*b*) Experimental histogram: the interaction forces between proteins A and B (black arrow) plus non-specific forces (yellow triangle and dashed black arrows) of all the construct components are measured, giving a force histogram that includes both kinds of interaction. (*c*) The unspecific interactions are filtered using the control histogram force, obtaining only the forces of the interaction between the two proteins.

(1) The lifetime of interaction τ_0, whose reciprocal corresponds to the dissociation kinetic constant, k_{off}.
(2) The free energy difference to the transition state $\Delta G^{\neq}$, which corresponds to the energy barrier for the dissociation process.
(3) The distance to the transition state $\Delta x^{\neq}$, which correlates with the interactions that must be broken to separate the two molecules (Schlierf and Rief, 2005; Tych *et al.*, 2013; Stigler and Rief, 2015).

The scaling factor ν can be adjusted to values $\nu = 1/2$ for a harmonic oscillator, $\nu = 2/3$ for a potential with linear and cubic terms, and $\nu = 1$ for an exponential known as the Bell equation (Bell, 1978). For this last case, where $\tau(F) = \tau_0 e^{-\beta F \Delta x^{\neq}}$, it is not possible to obtain values of $\Delta G^{\neq}$.

Force ramp in cis *interaction strategy*

Interaction lifetimes can be assigned to each bar of the rupture force histogram (Eq. (7)). A non-linear regression of lifetime *versus* force graph, given by the DHS model (Eq. (9)), is used to obtain the kinetic parameters of dissociation process.

Sometimes, non-specific interactions (i.e. every interaction between the components of the system that are not the two molecules of interest at their specific interaction site) can mask the specific interaction of interest. In this case, multimodal force ramp histograms are common, with a very high number of forces ramp below 10 pN (Fig. 4*b*). In the next section, a statistical analysis method will be revised in order to filter the specific data and to dampen the effect of non-specific interactions on the kinetic parameters obtained.

Methodology to obtain the specific interaction forces between the molecules of interest

Let us call our molecules of interest *A* and *B*. In an ideal scenario, only interactions between *A* and *B* would be measured; let us call these events *AB*. However, in a real experiment, a lot of rupture events are observed that do not correspond to *AB*-interactions, these can be from interactions of our molecules of interest directly with the beads and/or other molecules in the environment. Let us call these events AB. If only *AB*-events are of interest, but some of our measurements are AB, is there a way to obtain the rupture-force distribution of *AB*-events?

https://doi.org/10.1017/S0033583522000075 Published online by Cambridge University Press

A reasonable assumption is that both events are mutually exclusive. A rupture event cannot belong to a specific (AB) and non-specific ($\underline{AB}$) interaction at the same time. Another reasonable assumption is that both events are complementary, so that only specific or non-specific interactions can be observed (as only data where interactions were observed are collected), so

$$P(\underline{AB}) + P(AB) = 1. \tag{10}$$

This allows us to relate the probability $P(F)$ of a rupture event happening between F and $F + \mathrm{d}F$ to its conditional probabilities:

$$P(F) = P(F|AB) \cdot P(AB) + P(F|\underline{AB}) \cdot P(\underline{AB}). \tag{11}$$

The probability $P(F|\underline{AB})$ corresponds experimentally to the rupture-force histogram when there are no specific interactions. This scenario can be achieved when the molecules A and B are not present. $P(F)$ is the rupture-force histogram when A and B are present and there are other molecules that can interfere with the measurement of AB-events.

Finally, to reconstruct the rupture-force distribution for AB-events, Bayes' theorem can be used to obtain the expected proportion of AB to $\underline{AB}$ events for a given force

$$\frac{P(AB|F)}{P(\underline{AB}|F)} = \frac{P(AB)P(F|AB)}{P(\underline{AB})P(F|\underline{AB})} \tag{12}$$

and can be used to create an 'experimental' rupture-force histogram for AB-events. The method can be summarized as follows:

(1) Characterize the non-specific background by measuring without the presence of molecules of interest, effectively an experimental $P(F|\underline{AB})$. Then fit to the cumulative distribution function (CDF) in order to have a continuous expression for $P(F|\underline{AB})$. Smoothing is also a viable alternative (Fig. 4*a*).
(2) Introduce molecules A and B to the system. By measuring the rupture-force histogram, obtain an experimental $P(F)$. By fitting to the CDF and using Eq. (2), obtain $P(AB) = 1 - P(\underline{AB})$ and an expression for $P(F|AB)$ (Fig. 4*b*).
(3) Finally, by computing the ratio in Eq. (3) and using it to weigh the points that go into the rupture-force histogram $P(F)$, reconstruct an experimental histogram associated to AB-events (Fig. 4*c*).

If necessary, proper modeling of $P(F|AB)$ can be done assuming that it has a DHS-determined shape. In principle, the models used for $P(F|AB)$ and $P(F|\underline{AB})$ are not critical as long as AB events can be clearly distinguished in the fit of the experimental cumulative distribution of $P(F)$ (which would be characterized by a small fit error on $P(AB)$). In practice, this will be achieved if (1) the rupture-force histograms of the molecules of interest have distinguishably different behavior compared to the background and/or (2) a large amount of data was taken, improving the statistical error on $P(AB)$. An example where this problem is easy to see is when the AB events behave exactly like the background. Then this method would not give a reasonable result, and the error on $P(AB)$ will be nonsensically large (note that $P(AB)$ can only be from 0 to 1).

Once the filtered force histogram has been obtained, the DHS model is applied to calculate the biochemical parameters (see Section 'Obtaining biochemical parameters through the DHS model').

Finally, it is possible to apply the Jarzynski equality (Jarzynski, 1997), which allows us to obtain the free energy of the associated and dissociated state between both proteins, allowing the kinetic parameters of association to be explored indirectly, if there are no intermediates in this process (Raman *et al.*, 2014).

Conclusions

As shown in this review, it is possible to characterize protein–protein interactions in great detail at the single-molecule level. We showed three different configurations used in OT experiments that can be used to measure the biophysical parameters of the interaction (refolding and unfolding in *trans* interaction; constant force in *cis* interaction; force ramp in *cis* interaction).

Using the outlined methods, it is possible to obtain parameters like kinetics constants (k_{off}, k_{on}), affinity values (K_D), energy to the transition state $\Delta G^{\neq}$, and distance to the transition state $\Delta x^{\neq}$, providing a thorough characterization of the energy landscape of the interaction. Furthermore, some parameters such as distance to the transition state are only obtained from force spectroscopy experiments.

Also, a methodology to obtain the specific interaction forces between the molecules of interest is detailed. The interesting thing about this presented technique is that through experimental controls and mathematical analysis, non-specific interactions can be distinguished from specific interactions.

Currently, new OT instruments are appearing that allow changes in temperature in the experimental chamber (de Lorenzo *et al.*, 2015). With those instruments we will have a more complete view of the energy landscape of the interaction and obtain other parameters such as specific heat. Finally, newer models are appearing that consider more complete range of forces and higher pulling speed such as Bullerjahn–Sturm–Kroy model (Bullerjahn *et al.*, 2014) and Cossio–Hummer–Szabo (CHS) model (Cossio *et al.*, 2016). These will make it possible to determine with greater precision the intermolecular interactions at the single molecule. Other parameters will become attainable, such as critical force (F_c; force at which the energy barrier disappears; Bullerjahn *et al.*, 2014) and the μ parameter that indicates kinetic ductility of the protein (Cossio *et al.*, 2016). Both experimental advances and theoretical analyses must intertwine and develop together. As presented in this work, both the experimental part and mathematical analysis are important for an optimal analysis of the observed phenomena.

Acknowledgments. This work was supported by: FONDECYT 1181361, PCI PII20150073 (C.A.M.W.). The authors are thankful for interactions with all members of Biochemistry Laboratory of the Universidad de Chile. Additionally, the authors thank Ms. Shantanu Kadam, Fernando Medina, and Virginia Rusell for their critical proofreading of the manuscript.

References

Akasaka K, Kitahara R and Kamatari YO (2013) Exploring the folding energy landscape with pressure. *Archives of Biochemistry and Biophysics* **531**, 110–115.

Akiyoshi B, Sarangapani KK, Powers AF, Nelson CR, Reichow SL, Arellano-Santoyo H, Gonen T, Ranish JA, Asbury CL, and Biggins S (2010) Tension directly stabilizes reconstituted kinetochore-microtubule attachments. *Nature* **468**, 576–579.

Allen S, Chen X, Davies J, Davies MC, Dawkes AC, Edwards JC, Roberts CJ, Sefton J, Tendler SJB, and Williams PM (1997) Detection of antigen–

https://doi.org/10.1017/S0033583522000075 Published online by Cambridge University Press

antibody binding events with the atomic force microscope. *Biochemistry* **36**, 7457–7463.

Alon R, Hammer DA and Springer TA (1995) Lifetime of the P-selectin-carbohydrate bond and its response to tensile force in hydrodynamic flow. *Nature* **374**, 539–542.

Ananthakrishnan R and Ehrlicher A (2007) The forces behind cell movement. *International Journal of Biological Sciences* **3**, 303–317.

Ashkin A (1970) Acceleration and trapping of particles by radiation pressure. *Physical Review Letters* **24**, 156–159.

Aubin-Tam M-E, Olivares AO, Sauer RT, Baker TA and Lang MJ (2011) Single-molecule protein unfolding and translocation by an ATP-fueled proteolytic machine. *Cell* **145**, 257–267.

Avellaneda MJ, Koers EJ, Minde DP, Sunderlikova V and Tans SJ (2020) Simultaneous sensing and imaging of individual biomolecular complexes enabled by modular DNA–protein coupling. *Communications Chemistry* **3**, 20.

Baez M, Wilson CAM, Ramírez-Sarmiento CA, Guixé V and Babul J (2012) Expanded monomeric intermediate upon cold and heat unfolding of phosphofructokinase-2 from *Escherichia coli*. *Biophysical Journal* **103**, 2187–2194.

Bartels FW, Baumgarth B, Anselmetti D, Ros R and Becker A (2003) Specific binding of the regulatory protein ExpG to promoter regions of the galactoglucan biosynthesis gene cluster of *Sinorhizobium meliloti* – a combined molecular biology and force spectroscopy investigation. *Journal of Structural Biology* **143**, 145–152.

Bartels FW, McIntosh M, Fuhrmann A, Metzendorf C, Plattner P, Sewald N, Anselmetti D, Ros R and Becker A (2007) Effector-stimulated single molecule protein–DNA interactions of a quorum-sensing system in *Sinorhizobium meliloti*. *Biophysical Journal* **92**, 4391–4400.

Baumgarth B, Bartels FW, Anselmetti D, Becker A and Ros R (2005) Detailed studies of the binding mechanism of the *Sinorhizobium meliloti* transcriptional activator ExpG to DNA. *Microbiology* **151**, 259–268.

Bell GI (1978) Models for the specific adhesion of cells to cells. *Science* **200**, 618–627.

Björnham O and Schedin S (2009) Methods and estimations of uncertainties in single-molecule dynamic force spectroscopy. *European Biophysics Journal* **38**, 911–922.

Block SM, Goldstein LSB and Schnapp BJ (1990) Bead movement by single kinesin molecules studied with optical tweezers. *Nature* **348**, 348–352.

Bouchiat C, Wang MD, Allemand JF, Strick T, Block SM and Croquette V (1999) Estimating the persistence length of a worm-like chain molecule from force–extension measurements. *Biophysical Journal* **76**, 409–413.

Brampton C, Wahab O, Batchelor MR, Allen S and Williams PM (2011) Biomembrane force probe investigation of RNA dissociation. *European Biophysics Journal* **40**, 247–257.

Bullerjahn JT, Sturm S and Kroy K (2014) Theory of rapid force spectroscopy. *Nature Communications* **5**, 4463.

Burgos-Bravo F, Figueroa NL, Casanova-Morales N, Quest AFG, Wilson CAM and Leyton L (2018) Single-molecule measurements of the effect of force on Thy-1/$\alpha v\beta 3$-integrin interaction using nonpurified proteins. *Molecular Biology of the Cell* **29**, 326–338. doi: 10.1091/mbc.E17-03-0133.

Burgos-Bravo F, Martínez-Meza S, Quest AFG, Wilson CAM and Leyton L (2020) Application of force to a syndecan-4 containing complex with Thy-1–$\alpha V\beta 3$ integrin accelerates neurite retraction. *Frontiers in Molecular Biosciences* **7**. doi: 10.3389/fmolb.2020.582257

Bustamante C (2008) *In singulo* biochemistry: when less is more. *Annual Review of Biochemistry* **77**, 45–50.

Bustamante C and Smith S (2007) Optical beam translation device and method utilizing a pivoting optical fiber. Patent No.: US 7,274,451 B2.

Bustamante C, Bryant Z and Smith SB (2003) Ten years of tension: single-molecule DNA mechanics. *Nature* **421**, 423–427.

Bustamante C, Chemla YR, Forde NR and Izhaky D (2004) Mechanical processes in biochemistry. *Annual Review of Biochemistry* **73**, 705–748.

Bustamante A, Sotelo-Campos J, Guerra DG, Wilson CAM, Bustamante C and Báez M (2017) The energy cost of polypeptide knot formation and its folding consequences. *Nature Communications* **8**, 1581.

Cai X-E and Yang J (2003) The binding potential between the cholera toxin B-oligomer and Its receptor. *Biochemistry* **42**, 4028–4034.

Casanova-Morales N, Alavi Z, Wilson CAM and Zocchi G (2018*a*) Identifying chaotropic and kosmotropic agents by nanorheology. *Journal of Physical Chemistry B* **122**, 3754–3759. doi:10.1021/acs.jpcb.7b12782.

Casanova-Morales N, Quiroga-Roger D, Alfaro-Valdés HM, Alavi Z, Lagos-Espinoza MIA, Zocchi G, Wilson CAM (2018*b*) Mechanical properties of BiP protein determined by nano-rheology. *Protein Science* **27**, 1418–1426.

Casanova-Morales N, Figueroa NL, Alfaro K, Montenegro F, Barrera NP, Maze JR, Wilson CAM and Conejeros P (2019) Structural characterization of the saxitoxin-targeting APTSTX1 aptamer using optical tweezers and molecular dynamics simulations. *PLoS ONE* **14**, e0222468.

Cecconi C, Shank EA, Dahlquist FW, Marqusee S and Bustamante C (2008) Protein–DNA chimeras for single molecule mechanical folding studies with the optical tweezers. *European Biophysics Journal* **37**, 729–738.

Cecconi C, Shank EA, Marqusee S and Bustamante C (2011) DNA molecular handles for single-molecule protein-folding studies by optical tweezers, pp. 255–271.

Chen W, Lou J and Zhu C (2010) Forcing switch from short- to intermediate- and long-lived states of the αA domain generates LFA-1/ICAM-1 catch bonds. *Journal of Biological Chemistry* **285**, 35967–35978.

Chen K, He Y, Srinivasakannan C, Li S, Yin S, Peng J, Guo S and Zhang L (2019) Characterization of the interaction of rare earth elements with P507 in a microfluidic extraction system using spectroscopic analysis. *Chemical Engineering Journal* **356**, 453–460.

Claudia D, Greenfield D and Prentiss M (2005) Dissociation of ligand–receptor complexes using magnetic tweezers. doi:10.1021/AC050057+.

Comstock MJ, Ha T and Chemla YR (2011) Ultrahigh-resolution optical trap with single-fluorophore sensitivity. *Nature Methods* **8**, 335–340.

Cossio P, Hummer G and Szabo A (2016) Kinetic ductility and force-spike resistance of proteins from single-molecule force spectroscopy. *Biophysical Journal* **111**, 832–840.

Dague E, Pons V, Roland A, Azaïs JM, Arcucci S, Lachaize V, Velmont S, Trevisiol E, N'Guyen D, Sénard JM and Galés C (2022) Atomic force microscopy-single-molecule force spectroscopy unveils GPCR cell surface architecture. *Communications Biology* **5**, 1–13.

Dammer U, Popescu O, Wagner P, Anselmetti D, Guntherodt H and Misevic G (1995) Binding strength between cell adhesion proteoglycans measured by atomic force microscopy. *Science* **267**, 1173–1175.

Danilowicz C, Greenfield D, Prentiss M (2005) Dissociation of ligand–receptor complexes using magnetic tweezers. *Analytical Chemistry* **77**, 3023–3028.

de Lorenzo S, Ribezzi-Crivellari M, Arias-Gonzalez JR, Smith SB and Ritort F (2015) A temperature-jump optical trap for single-molecule manipulation. *Biophysical Journal* **108**, 2854–2864.

Dembo M, Torney DC, Saxman K and Hammer D (1988) The reaction-limited kinetics of membrane-to-surface adhesion and detachment. *Proceedings of the Royal Society of London. Series B. Biological Sciences* **234**, 55–83.

Desai VP, Frank F, Lee A, Righini M, Lancaster L, Noller HF, Tinoco I and Bustamante C (2019) Co-temporal force and fluorescence measurements reveal a ribosomal gear shift mechanism of translation regulation by structured mRNAs. *Molecular Cell* **75**, 1007–1019.e5.

Dudko OK, Hummer G and Szabo A (2008) Theory, analysis, and interpretation of single-molecule force spectroscopy experiments. *Proceedings of the National Academy of Sciences* **105**, 15755–15760.

Eckel R, Ros R, Decker B, Mattay J and Anselmetti D (2005*a*) Supramolecular chemistry at the single-molecule level. *Angewandte Chemie International Edition* **44**, 484–488.

Eckel R, Wilking SD, Becker A, Sewald N, Ros R and Anselmetti D (2005*b*) Single-molecule experiments in synthetic biology: an approach to the affinity ranking of DNA-binding peptides. *Angewandte Chemie International Edition* **44**, 3921–3924.

Evans, E. and Kinoshita, K. (2007). Using force to probe single-molecule receptor–cytoskeletal anchoring beneath the surface of a living cell, pp. 373–396.

Evans E, Ritchie K and Merkel R (1995) Sensitive force technique to probe molecular adhesion and structural linkages at biological interfaces. *Biophysical Journal* **68**, 2580–2587.

Evans E, Leung A, Heinrich V and Zhu C (2004) Mechanical switching and coupling between two dissociation pathways in a P-selectin adhesion bond. *Proceedings of the National Academy of Sciences* **101**, 11281–11286.

https://doi.org/10.1017/S0033583522000075 Published online by Cambridge University Press

Evans E, Heinrich V, Leung A and Kinoshita K (2005) Nano- to microscale dynamics of P-selectin detachment from leukocyte interfaces. I. Membrane Separation from the Cytoskeleton. *Biophysical Journal* **88**, 2288–2298.

Evans E, Kinoshita K, Simon S and Leung A (2010) Long-lived, high-strength states of ICAM-1 bonds to β2 integrin, I: lifetimes of bonds to recombinant αLβ2 under force. *Biophysical Journal* **98**, 1458–1466.

Fillebeen C, Wilkinson N and Pantopoulos K (2014) Electrophoretic mobility shift assay (EMSA) for the study of RNA–protein interactions: the IRE/IRP example. *Journal of Visualized Experiments*. doi: 10.3791/52230

Fiore VF, Ju L, Chen Y, Zhu C and Barker TH (2014) Dynamic catch of a Thy-1–α5β1 + syndecan-4 trimolecular complex. *Nature Communications* **5**, 4886.

Florin E, Moy V and Gaub H (1994) Adhesion forces between individual ligand–receptor pairs. *Science* **264**, 415–417.

Forns N, de Lorenzo S, Manosas M, Hayashi K, Huguet JM and Ritort F (2011) Improving signal/noise resolution in single-molecule experiments using molecular constructs with short handles. *Biophysical Journal* **100**, 1765–1774.

Fournier MF, Sauser R, Ambrosi D, Meister J-J and Verkhovsky AB (2010) Force transmission in migrating cells. *Journal of Cell Biology* **188**, 287–297.

Fritz J, Katopodis AG, Kolbinger F and Anselmetti D (1998) Force-mediated kinetics of single P-selectin/ligand complexes observed by atomic force microscopy. *Proceedings of the National Academy of Sciences* **95**, 12283–12288.

Fuhrmann A and Ros R (2010) Single-molecule force spectroscopy: a method for quantitative analysis of ligand–receptor interactions. *Nanomedicine: Nanotechnology, Biology, and Medicine* **5**, 657–666.

Fuhrmann A, Schoening JC, Anselmetti D, Staiger D and Ros R (2009) Quantitative analysis of single-molecule RNA–protein interaction. *Biophysical Journal* **96**, 5030–5039.

Fukuda S, Yan S, Komi Y, Sun M, Gabizon R and Bustamante C (2020) The biogenesis of SRP RNA is modulated by an RNA folding intermediate attained during transcription. *Molecular Cell* **77**, 241–250.e8.

Ghisaidoobe A and Chung S (2014) Intrinsic tryptophan fluorescence in the detection and analysis of proteins: a focus on Förster resonance energy transfer techniques. *International Journal of Molecular Sciences* **15**, 22518–22538.

Gourier C, Jegou A, Husson J and Pincet F (2008) A nanospring named erythrocyte. The biomembrane force probe. *Cellular and Molecular Bioengineering* **1**, 263–275.

Guo H and Li Z (2013) Optical tweezers technique and its applications. *Science China Physics, Mechanics and Astronomy* **56**, 2351–2360.

Hackl M, Contrada EV, Ash JE and Chundawat SPS (2021) Acoustic force spectroscopy reveals subtle differences in cellulose unbinding behavior of carbohydrate-binding modules. *BioRxiv*, 2021.09.20.461102.

Halvorsen K, Schaak D and Wong WP (2011) Nanoengineering a single-molecule mechanical switch using DNA self-assembly. *Nanotechnology* **22**, 494005. doi:10.1088/0957-4484/22/49/494005.

Hinterdorfer P, Baumgartner W, Gruber HJ, Schilcher K and Schindler H (1996) Detection and localization of individual antibody-antigen recognition events by atomic force microscopy. *Proceedings of the National Academy of Sciences* **93**, 3477–3481.

Jarzynski C (1997) Nonequilibrium equality for free energy differences. *Physical Review Letters* **78**, 2690–2693.

Kada G, Blayney L, Jeyakumar L, Kienberger F, Pastushenko VPh, Fleischer S, Schindler H, Lai FA and Hinterdorfer P (2001) Recognition force microscopy/spectroscopy of ion channels: applications to the skeletal muscle Ca^{2+} release channel (RYR1). *Ultramicroscopy* **86**, 129–137.

Kaiser CM, Goldman DH, Chodera JD, Tinoco I and Bustamante C (2011) The ribosome modulates nascent protein folding. *Science* **334**, 1723–1727.

Kamsma D and Wuite GJL (2018) single-molecule measurements using acoustic force spectroscopy (AFS), pp. 341–351.

Kamsma D, Bochet P, Oswald F, Alblas N, Goyard S, Wuite GJL, Peterman EJG and Rose T (2018) Single-cell acoustic force spectroscopy: resolving kinetics and strength of T cell adhesion to fibronectin. *Cell Reports* **24**, 3008–3016.

Kienberger F, Kada G, Mueller H and Hinterdorfer P (2005) Single molecule studies of antibody–antigen interaction strength versus intra-molecular antigen stability. *Journal of Molecular Biology* **347**, 597–606.

Kilinc D, Blasiak A, O'Mahony JJ, Suter DM and Lee GU (2012) Magnetic tweezers-based force clamp reveals mechanically distinct apCAM domain interactions. *Biophysical Journal* **103**, 1120–1129.

Kim J, Zhang C-Z, Zhang X and Springer TA (2010) A mechanically stabilized receptor–ligand flex-bond important in the vasculature. *Nature* **466**, 992–995.

Kim J, Hudson NE and Springer TA (2015) Force-induced on-rate switching and modulation by mutations in gain-of-function von Willebrand diseases. *Proceedings of the National Academy of Sciences* **112**, 4648–4653.

Kokkoli E, Ochsenhirt SE and Tirrell M (2004) Collective and single-molecule interactions of α5β1 integrins. *Langmuir* **20**, 2397–2404.

Kühner F, Costa LT, Bisch PM, Thalhammer S, Heckl WM and Gaub HE (2004) LexA–DNA bond strength by single molecule force spectroscopy. *Biophysical Journal* **87**, 2683–2690.

Lavoisier A (1790) Elements of chemistry: in a new systematic order, containing all the modern discoveries.

Lee I and Marchant RE (2001) Force measurements on the molecular interactions between ligand (RGD) and human platelet αIIbβ3 receptor system. *Surface Science* **491**, 433–443.

Lee I and Marchant RE (2003) Molecular interaction studies of hemostasis: fibrinogen ligand–human platelet receptor interactions. *Ultramicroscopy* **97**, 341–352.

Lee G, Chrisey L and Colton R (1994*a*) Direct measurement of the forces between complementary strands of DNA. *Science* **266**, 771–773.

Lee GU, Kidwell DA and Colton RJ (1994*b*) Sensing discrete streptavidin-biotin interactions with atomic force microscopy. *Langmuir* **10**, 354–357.

Lee C-Y, Lou J, Wen K-K,McKane M, Eskin S G, Ono S, Chien S, Rubenstein PA, Zhu C, McIntire LV (2013) Actin depolymerization under force is governed by lysine 113:glutamic acid 195-mediated catch-slip bonds. *Proceedings of the National Academy of Sciences* **110**, 5022–5027.

Li P, Jiang N, Nagarajan S, Wohlhueter R, Selvaraj P and Zhu C (2007) Affinity and kinetic analysis of Fcγ receptor IIIa (CD16a) binding to IgG ligands. *Journal of Biological Chemistry* **282**, 6210–6221.

Lin S-N, Qin L, Wuite GJL and Dame RT (2018) Unraveling the biophysical properties of chromatin proteins and DNA using acoustic force spectroscopy, **1837**, 301–316.

Litvinov RI, Bennett JS, Weisel JW and Shuman H (2005) Multi-step fibrinogen binding to the integrin αIIbβ3 detected using force spectroscopy. *Biophysical Journal* **89**, 2824–2834.

Lo Y-S, Zhu Y-J and Beebe TP (2001) Loading-Rate dependence of individual ligand–receptor bond-rupture forces studied by atomic force microscopy. *Langmuir* **17**, 3741–3748.

Lynch S, Baker H, Byker SG, Zhou D and Sinniah K (2009) Single molecule force spectroscopy on G-quadruplex DNA. *Chemistry – A European Journal* **15**, 8113–8116.

Marshall BT, Long M, Piper JW, Yago T, McEver RP and Zhu C (2003) Direct observation of catch bonds involving cell-adhesion molecules. *Nature* **423**, 190–193.

Mateluna C, Torres P, Rodriguez–Peña M, Silva P, Matthies DJ, Criollo A, Bikker FJ, Bolscher JGM, Wilson CAM, Zapata–Torres G and Torres VA (2022) Identification of VEGFR2 as the histatin-1 receptor in endothelial cells. *Biochemical Pharmacology* **201**, 115079.

Mejean CO, Schaefer AW, Millman EA, Forscher P and Dufresne ER (2009) Multiplexed force measurements on live cells with holographic optical tweezers. *Optics Express* **17**, 6209.

Merkel R, Nassoy P, Leung A, Ritchie K and Evans E (1999) Energy landscapes of receptor–ligand bonds explored with dynamic force spectroscopy. *Nature* **397**, 50–53.

Meyer G and Amer NM (1988) Novel optical approach to atomic force microscopy. *Applied Physics Letters* **53**, 1045–1047.

Misselwitz B, Staeck O and Rapoport TA (1998) J proteins catalytically activate Hsp70 molecules to trap a wide range of peptide sequences. *Molecular Cell* **2**, 593–603.

Molloy JE and Padgett MJ (2002) Lights, action: optical tweezers. *Contemporary Physics* **43**, 241–258.

https://doi.org/10.1017/S0033583522000075 Published online by Cambridge University Press

Morfill J, Blank K, Zahnd C, Luginbühl B, Kühner F, Gottschalk K-E, Plückthun A and Gaub HE (2007) Affinity-matured recombinant antibody fragments analyzed by single-molecule force spectroscopy. *Biophysical Journal* **93**, 3583–3590.

Muñoz R, Aguilar Sandoval F, Wilson CAM and Melo F (2015) Pulling on super paramagnetic beads with micro cantilevers: single molecule mechanical assay application. *Physical Biology* **12**, 046011.

Neuman KC and Nagy A (2008) Single-molecule force spectroscopy: optical tweezers, magnetic tweezers and atomic force microscopy. *Nature Methods* **5**, 491–505.

Nicholas MP, Rao L and Gennerich A (2014) An improved optical tweezers assay for measuring the force generation of single kinesin molecules. *Methods in Molecular Biology* **1136**, 171–246.

Nieminen TA, Knöner G, Heckenberg NR and Rubinsztein-Dunlop H (2007) Physics of Optical Tweezers, pp. 207–236.

Nishizaka T, Tadakuma H, Kato H, Miyata H and Kinosita KSI (1996) *Lifetime of a single actomyosin rigor bond measured using optical tweezers.*

Nobel Prize (2021) Arthur Ashkin. Available at https://www.nobelprize.org/prizes/physics/2018/ashkin/.

O'Shannessy DJ (1994) Determination of kinetic rate and equilibrium binding constants for macromolecular interactions: a critique of the surface plasmon resonance literature. *Current Opinion in Biotechnology* **5**, 65–71.

Peña-Oyarzun D, Rodriguez-Peña M, Burgos-Bravo F,Vergara A, Kretschmar C, Sotomayor-Flores C, Ramirez-Sarmiento CA, De Smedt H, Reyes M, Perez W, Torres V A, Morselli E, Altamirano F, Wilson C AM, Hill J A, Lavandero S, Criollo A (2020) PKD2/polycystin-2 induces autophagy by forming a complex with BECN1. *Autophagy* **17**(7), 1714–1728.

Perret E, Leung A, Feracci H and Evans E (2004) Trans-bonded pairs of E-cadherin exhibit a remarkable hierarchy of mechanical strengths. *Proceedings of the National Academy of Sciences* **101**, 16472–16477.

Pierres A, Touchard D, Benoliel A-M and Bongrand P (2002) Dissecting streptavidin–biotin interaction with a laminar flow chamber. *Biophysical Journal* **82**, 3214–3223.

Pierres A, Benoliel A-M and Bongrand P (2008) Studying molecular interactions at the single bond level with a laminar flow chamber. *Cellular and Molecular Bioengineering* **1**, 247–262.

Polacheck WJ, Charest JL and Kamm RD (2011) Interstitial flow influences direction of tumor cell migration through competing mechanisms. *Proceedings of the National Academy of Sciences* **108**, 11115–11120.

Polimeno P, Magazzù A, Iatì MA, Patti F, Saija R, Esposti B C D, Donato M G, Gucciardi P G, Jones P H, Volpe G,Maragò OM (2018) Optical tweezers and their applications. *Journal of Quantitative Spectroscopy and Radiative Transfer* **218**, 131–150.

Pollard TD and Borisy GG (2003) Cellular motility driven by assembly and disassembly of actin filaments. *Cell* **112**, 453–465.

Porter-Peden L, Kamper SG, Vander Wal M, Blankespoor R and Sinniah K (2008) Estimating kinetic and thermodynamic parameters from single molecule enzyme–inhibitor interactions. *Langmuir* **24**, 11556–11561.

Rakshit S, Zhang Y, Manibog K, Shafraz O and Sivasankar S (2012) Ideal, catch, and slip bonds in cadherin adhesion. *Proceedings of the National Academy of Sciences* **109**, 18815–18820.

Raman S, Utzig T, Baimpos T, Ratna Shrestha B and Valtiner M (2014) Deciphering the scaling of single-molecule interactions using Jarzynski's equality. *Nature Communications* **5**, 5539.

Ramírez MP (2016) *Studying the role of BiP as a chaperone through single*, Universidad de Chile.

Ramírez MP, Rivera M, Quiroga-Roger D, Bustamante A, Vega M, Baez M, Puchner E M,Wilson CAM (2017) Single molecule force spectroscopy reveals the effect of BiP chaperone on protein folding. *Protein Science* **26**, 1404–1412.

Rinko LJ, Lawrence MB and Guilford WH (2004) The molecular mechanics of P- and L-selectin lectin domains binding to PSGL-1. *Biophysical Journal* **86**, 544–554.

Robert P, Benoliel A-M, Pierres A and Bongrand P (2007) What is the biological relevance of the specific bond properties revealed by single-molecule studies? *Journal of Molecular Recognition* **20**, 432–447.

Rognoni L, Stigler J, Pelz B, Ylanne J and Rief M (2012) Dynamic force sensing of filamin revealed in single-molecule experiments. *Proceedings of the National Academy of Sciences* **109**, 19679–19684.

Schlierf M and Rief M (2005) Temperature softening of a protein in single-molecule experiments. *Journal of Molecular Biology* **354**, 497–503.

Schmid D, Baici A, Gehring H and Christen P (1994) Kinetics of molecular chaperone action. *Science* **263**, 971–973.

Shang H and Lee GU (2007) Magnetic tweezers measurement of the bond lifetime–force behavior of the IgG – protein A specific molecular interaction. *Journal of the American Chemical Society* **129**, 6640–6646.

Shao J-Y (2004) Quantifying cell-adhesion strength with micropipette manipulation: principle and application. *Frontiers in Bioscience* **9**, 2183.

Shemesh J, Jalilian I, Shi A, Heng Yeoh G, Knothe Tate ML and Ebrahimi Warkiani M (2015) Flow-induced stress on adherent cells in microfluidic devices. *Lab on a Chip* **15**, 4114–4127.

Singha Roy A, Dinda AK, Chaudhury S and Dasgupta S (2014) Binding of antioxidant flavonol morin to the native state of bovine serum albumin: effects of urea and metal ions on the binding. *Journal of Luminescence* **145**, 741–751.

Sitters G, Kamsma D, Thalhammer G, Ritsch-Marte M, Peterman EJG and Wuite GJL (2014) Acoustic force spectroscopy. *Nature Methods* **12**, 47–50.

Smith SB, Cui Y and Bustamante C (2003) Optical-trap force transducer that operates by direct measurement of light momentum. *Methods Enzymol* **361**, 134–162. doi:10.1016/s0076-6879(03)61009-8.

Sorkin R, Bergamaschi G, Kamsma D, Brand G, Dekel E, Ofir-Birin Y, Rudik A, Gironella M, Ritort F, Regev-Rudzki N, Roos W H, Wuite GJL (2018) Probing cellular mechanics with acoustic force spectroscopy. *Molecular Biology of the Cell* **29**, 2005–2011.

Stangner T, Wagner C, Singer D,Angioletti-Uberti S, Gutsche C, Dzubiella J, Hoffmann R, Kremer F (2013) Determining the specificity of monoclonal antibody HPT-101 to tau-peptides with optical tweezers. *ACS Nano* **7**, 11388–11396.

Stigler J and Rief M (2015) Ligand-induced changes of the apparent transition-state position in mechanical protein unfolding. *Biophysical Journal* **109**, 365–372.

Stout AL (2001) Detection and characterization of individual intermolecular bonds using optical tweezers. *Biophysical Journal* **80**, 2976–2986.

Sudhakar S, Abdosamadi MK, Jachowski TJ, Bugiel M, Jannasch A and Schäffer E (2021) Germanium nanospheres for ultraresolution picotensiometry of kinesin motors. *Science* **371**(6530). doi:10.1126/science.abd9944.

Sung K, Sung L, Crimmins M, Burakoff S and Chien S (1986) Determination of junction avidity of cytolytic T cell and target cell. *Science* **234**, 1405–1408.

Szili EJ, Al-Bataineh SA, Ruschitzka P,Desmet G, Priest C, Griesser HJ, Voelcker NH, Harding FJ, Steele DA, Short RD (2012) Microplasma arrays: a new approach for maskless and localized patterning of materials surfaces. *RSC Advances* **2**, 12007.

Thoumine O, Bard L, Saint-Michel E, Dequidt C and Choquet D (2008) Optical tweezers and fluorescence recovery after photo-bleaching to measure molecular interactions at the cell surface. *Cellular and Molecular Bioengineering* **1**, 301–311.

Tinoco I (2004) Force as a useful variable in reactions: unfolding RNA. *Annual Review of Biophysics and Biomolecular Structure* **33**, 363–385.

Tinoco I, Sauer K, Wang JC, Puglisi JD, Harbison G and Rovnyak D (2013) *Physical Chemistry: Principles and Applications in Biological Sciences.*

Tych KM, Hoffmann T, Brockwell DJ and Dougan L (2013) Single molecule force spectroscopy reveals the temperature-dependent robustness and malleability of a hyperthermophilic protein. *Soft Matter* **9**, 9016.

Ungai-Salánki R, Peter B, Gerecsei T, Orgovan N, Horvath R and Szabó B (2019) A practical review on the measurement tools for cellular adhesion force. *Advances in Colloid and Interface Science* **269**, 309–333.

Van Rosmalen MGM, Kamsma D, Biebricher AS, Li C, Zlotnick A, Roos WH and Wuite GJL (2020) Revealing in real-time a multistep assembly mechanism for SV40 virus-like particles. *Science Advances* **6**. doi:10.1126/sciadv.aaz1639.

Weisel J (2003) Protein–protein unbinding induced by force: single-molecule studies. *Current Opinion in Structural Biology* **13**, 227–235.

Whitley KD, Comstock MJ and Chemla YR (2017) High-Resolution 'Fleezers': Dual-Trap Optical Tweezers Combined with Single-Molecule Fluorescence Detection, pp. 183–256.

https://doi.org/10.1017/S0033583522000075 Published online by Cambridge University Press

Willemsen OH, Snel MME, Cambi A, Greve J, De Grooth BG and Figdor CG (2000) Biomolecular interactions measured by atomic force microscopy. *Biophysical Journal* **79**, 3267–3281.

Wilson C (2011) *Single Molecule Studies by Optical Tweezers: Folding and Unfolding of Glucokinase from Thermococcus litoralis*. Santiago, Chile: Universidad de Chile.

Yuan C, Chen A, Kolb P and Moy VT (2000) Energy landscape of streptavidin–biotin complexes measured by atomic force microscopy. *Biochemistry* **39**, 10219–10223.

Zaltron A, Merano M, Mistura G, Sada C and Seno F (2020) Optical tweezers in single-molecule experiments. *The European Physical Journal Plus* **135**, 896.

Zhang H and Liu K-K (2008) Optical tweezers for single cells. *Journal of the Royal Society Interface* **5**, 671–690.

Zhang X, Wojcikiewicz E and Moy VT (2002) Force spectroscopy of the leukocyte function-associated antigen-1/intercellular adhesion molecule-1 interaction. *Biophysical Journal* **83**, 2270–2279.

Zhu C (2014) Mechanochemitry: a molecular biomechanics view of mechanosensing. *Annals of Biomedical Engineering* **42**, 388–404.

Zohra FT (2021) Using single-molecule DNA flow-stretching experiments to see the effects of temperature and viscosity, The University of Texas Rio Grande Valley. Available at https://www.proquest.com/docview/2595580864?pq-origsite=gscholar&fromopenview=true.

https://doi.org/10.1017/S0033583522000075 Published online by Cambridge University Press